MEE 10:80

On Sphere detection for OFDM based MIMO systems

MD. SHAMSER ALAM

This thesis is presented as part of Degree of
Master of Science in Electrical Engineering

Blekinge Institute of Technology
September 2010

Blekinge Institute of Technology
School of Engineering
Department of Applied Signal Processing
Supervisor: Dr. Jörgen Nordberg
Examiner: Dr. Jörgen Nordberg

Abstract

The mobile wireless communication systems has been growing fast and continuously over the past two decades. Therefore, in order to fulfill the demand for this rapid growth, the standardization bodies along with wireless researchers and mobile operators around the world have been constantly working on new technical specifications.An important problem in modern communication is known as NP complete problem in the Maximum Likelihood (ML) detection of signals transmitting over Multiple Input Multiple Output channel of the OFDM transceiver system. Development of the Sphere Decoder (SD) as a result of the rapid advancement in signal processing techniques provides ML detection for MIMO channels at polynomial time complexity average case. There are weaknesses in the existing SDs. The sphere decoder performance is very sensitive for the most current proposals in order to choose the search radius parameter. At high spectral efficiencies SNR is low or as the problem dimension is high and the complexity coefficient can become very large too.

Digital communications of detecting a vector of symbols has importance as, is encountered in several different applications. These symbols are as the finite alphabet and transmitted over a multiple-input multiple-output (MIMO) channel with Gaussian noise. There are no limitation to the detection of symbols spatially multiplexed over a multiple-antenna channel and the multi user detection problem. Efficient algorithms are considered for the detection problems and have recognized well. The algorithm of sphere decoder, orders has optimal performance considering the error probability and this has proved extremely efficient in terms of computational complexity for moderately sized problems in case of signal to noise ratio. At high SNR the algorithm has a polynomial average complexity and it is understood the algorithm has an exponential worst case complexity. The efficiency of the algorithm is ordered the exponential rate derivation of growth. Complexity is positive for the finite SNR and small in the high SNR. To achieve the sphere decoding solution applying Schnorr-Euchner by Maximum likelihood method , Depth-first Stack-based Sequential decoding is used. This thesis focuses on the receiver part of the transceiver system and takes a good look at the near optimal algorithm for sphere detection of a vector of symbols transmitted over MIMO channel. The analysis and algorithms are general in nature.

Preface

I start with a few words of many acknowledgements on the hard work of research. Since I can think of few things equally rewarding, this is not one of those acknowledgements. Of course, research is not a one man show and without the help and encouragement of others, it can not be done. The work detailed in this report was undertaken as a component of my approved course of research for the master degree at the Blekinge Institute of Technology. My dissertation is tentatively entitled “On Sphere Detection for OFDM based MIMO System”.

First and foremost I would like to thank my supervisor, Professor Jorgen Nordberg, for his support and giving me the opportunity to work within the laboratory for communication engineering and sharing his knowledge and expertise. I am as grateful for the freedom to explore and dwell on all aspects of the problems which pass before me, as I am for the occasional nudge in right direction. There are numerous members of the signal processing and communication theory laboratories who contribute to the excellent working environment and creative atmosphere.

Finally, I most gratefully acknowledge the generous assistance of Blekinge Institute of Technology, Karlskrona, Sweden.

Md. Shamser Alam

Contents

List Of Figures

Chapter 1 Introduction

Wireless communications has emerged as one of the largest and most rapidly growing sectors of the global telecommunications industry driven by the demand for increasingly sophisticated connectivity at anytime and at anywhere .Communication by using Multiple Input Multiple Output (MIMO) antenna architectures [69] promises to play a key role in fuelling this tremendous growth which is one of the most significant technological developments of the last decade. The Universal Mobile Telecommunication System-Long Term Evolution (UMTS-LTE) has certain objectives to obtain the high data rate, low latency and optimized radio access technology [67,68] .Multiple element antenna arrays are deployed at both the transmitter and the receiver in a MIMO system. The communications challenge lies to the quality of the transmission (i.e., bit error probability) and/or its data rate that are superior in designing the sets of signals simultaneously sent by the transmit antennas and the algorithms for processing those observed by the receive antennas to those supported by traditional single antenna systems. Increased reliability, reduced power requirements and higher composite data rates can be provided by these gains. The specialty exciting about the benefits offered by MIMO technology is that these gains can be attained without the need for additional spectral resources, which are not only expensive but also extremely scarce. Particularly, signal detection has been the subject of intensive study at the receiver end of the MIMO channel .The Sphere Decoder (SD) [18, 19,13, 20, 21] is one of the most important and industrially relevant algorithms to emerge from these efforts. Optimal detection of signals or the Maximum Likelihood (ML) transmitted over MIMO channels is well-known to be an NP-complete problem [8,71]. Sphere decoding (SD) came into view as a challenging method to exhibit the optimum ML solution for the MIMO decoding problem which reformulates the impractical exhaustive search over all possible vectors that is transmitted into an efficient depth-first tree search. However, the complexity of the depth-first search involved by the SD algorithm is dependent on channel and noise conditions and the complexity can reach in the extreme condition of an exhaustive search. The Sphere Detection has been revealed to offer ML detection at a computational complexity which is polynomial in the average case [70]. Fincke-Pohst and Schnorr-Euchner enumerations can be considered as the basis of two Sphere Detection algorithms. The two enumeration strategies build up these schemes which are considered as the representative of the majority of existing decoders and so are used as my benchmarks.The greatly enhanced performance both theoretical and laboratory settings [12,15,16,17] have been shown over the last ten years. Hence Sphere Detection is the recent explosion of interest from both academic and industrial researchers in the area of signal processing techniques for MIMO systems.

1.1 The Detection Problem:

Existing Sphere Detection algorithms show two major weaknesses: First, the value chosen for the search radius parameter is highly sensitive for the performance of most

current proposals. The successful termination of the algorithm which provides the result of as an optimal solution, as well as its time complexity, are highly dependent on the search radius [18]. Secondly, the complexity coefficient can become very large when the SNR [11,12,13] is low, or when the problem dimension is high, e.g., at the high spectral efficiencies required to support higher communication rates, although its time complexity is polynomial in the average case .There are few detection problems in which the simultaneous detection of multiple users in a digital subscriber line (DSL) system affected by crosstalk [10] as the detection of symbols transmitted over the multi-user detection problem in the CDMA [7, 8, 9], multiple antenna wireless channel [1, 2, 3].

1.2 Ordinary Solution:

The detection algorithms are motivated and suboptimal research is computationally advantageous. The optimal, ML, detection problem is considered as to be NP-hard [8] which clearly indicates the polynomial complexity solutions are not obvious. The detection problem research in the last few years focuses on improving complex solutions and offers an acceptable probability of error performance. Grouping of detectors into classes is done as it is blurred to distinct between classes and so the detectors are placed in more than one class. The linear detector essentially only require a matrix vector multiplication but the error probability is typically much worse than that of the optimal detector. The linear detectors [23] are among the least computationally complex detectors when applied to the fading channel [3] or the channel matrix H is ranked deficient [24] where as the Decision Feedback Detectors [21,25,26,27,28]describe a nonlinear expansion of the linear detectors. Certain decisions are fed back into the detectors to get better results. However, the error of probability is occurred due to some decisions and limiting the quality of performance when applied to fading channels. Meanwhile, Error of probability provided by the feed back detectors decision over the linear counterpart increases the complexity marginally. At the end, relaxing the detection [29,30,31,32,33] problem does not necessarily lead to a large loss in terms of error probability. In fact, the main contribution shows that the SDR detector that achieves the maximal diversity in the real valued case when $n \geq m$. The lattice reduction [34,35,36,37,38] has the capability to improve the performance in terms of computational complexity and probability of many detectors. The suboptimal detectors performance is limited when faced with poorly conditioned channel matrices and the performance in terms of computational complexity, can be improved in some cases [13, 20].

1.3 Solution:

In this thesis, a simulation of the OFDM transceiver system [4,5] including the Sphere Detection is accomplished. For that purpose, a generic codeword Depth-first Stack-based sequential decoding Sphere Detector which is based respectively on both the Fincke-Pohst and Schnorr-Euchner enumerations was implemented to obtain the optimal solution. The tentative performance of the implemented OFDM transceiver is evaluated by different QAM modulations. The thesis for sphere detection of a vector of symbols transmitted over MIMO channel basically focuses on the receiver part of the transceiver

link. The sphere decoder's performance is sensitive to its radius parameter where as it is very important in the digital communication system to detect information that carries symbols transmitted over a communications channel with multiple inputs and multiple outputs .The analysis and algorithm are general in nature.

1.4 Thesis outline:

The first of my contributions introduces the sensitivity of the sphere decoder's performance to its radius parameter. In chapter 2, overview of the physical layer of the LTE system basically on OFDM based UMTS-LTE transmitter and receiver design structure with comprehensive details is illustrated where as the system model of the MIMO system is described in chapter 3 Chapter 4 details the basic concepts and fundamentals of mathematical implementation and the description of Sphere Decoding algorithm to find an ML solution in which the sensitivity of radius and its parameter are focused. In chapter 5 the performance of the designed system channel model is analyzed by different modulation techniques. Chapter 6 concludes this report on my work, which puts forward effective steps addressing the key issues both in sphere decoding and OFDM transceiver system, under certain conditions at a reduced time complexity.

Chapter 2 Overview of the physical layer of the LTE system

2.1 OFDM Transceiver:

Figure demonstrates the LTE design of the transmitter and receiver on the basis of physical layer information and the structure is based on OFDM system which depicts the implemented structure.

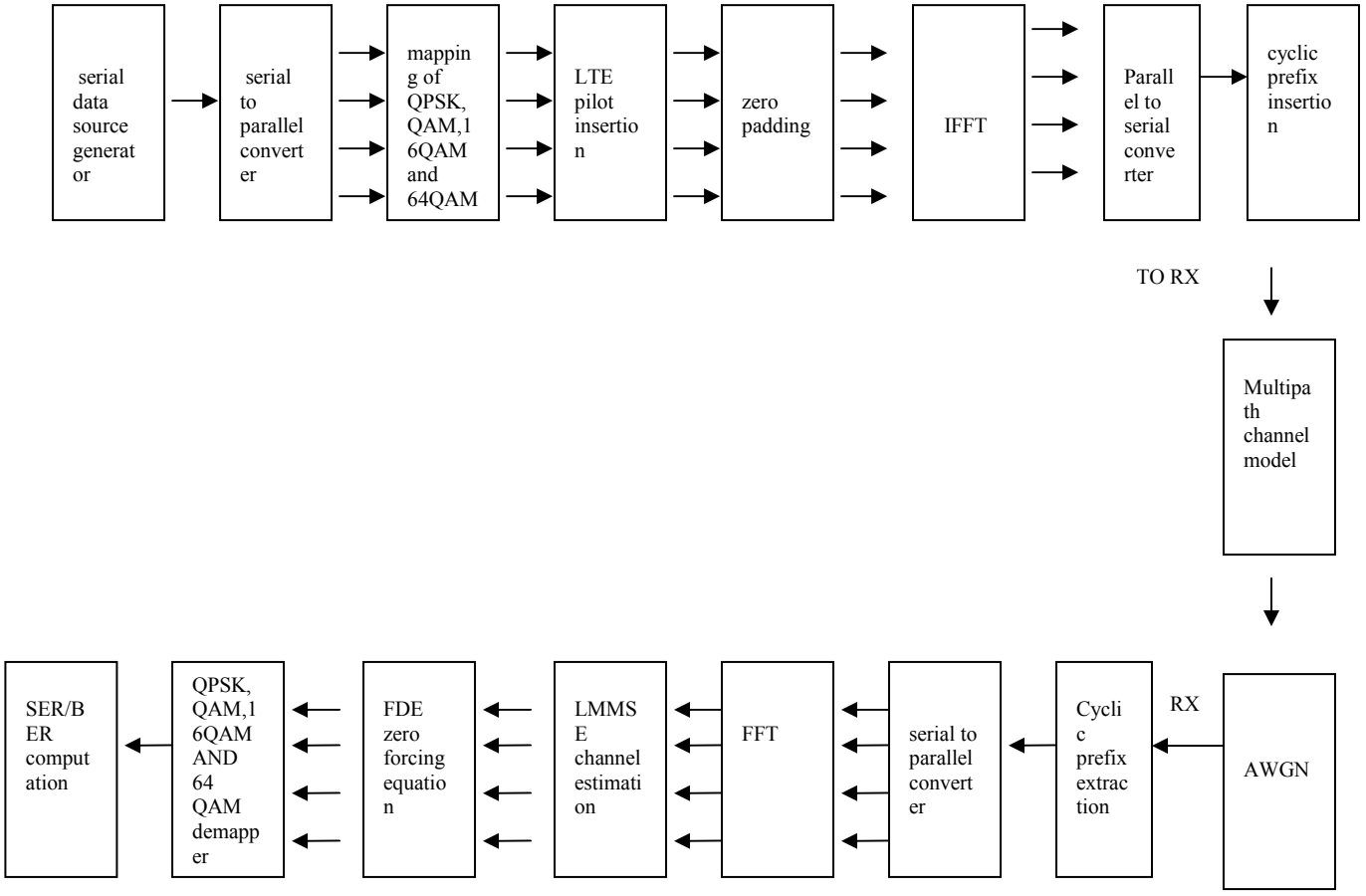

Fig2.1: Full Block structure for the UMTS-LTE Transceiver

2.2 Transmitter:

As the block diagram 2.2 describes the OFDM, UMTS-LTE transmitter structure. Here a 20 MHz bandwidth and the digital modulation are used to provide the feasibility required for the UMTS-LTE transmission chain. Generalized digital data is parallel and mapped into the complex block by modulation techniques. Symbol is referred as complex data block, and sub-carriers which is attached to data. The spectrum width is less than the sampling rate of the OFDM modulator as the unused bands are padded with zeros. Time version of signal is acquired by the IFFT and the time domain signals to all sub-carriers

are orthogonal to each other. The noise distortion and the inter symbol interference are the main drawback to the high data rate transmission. Frequency spectrums overlap in the process. Inter symbol interference is deleted as the signal duration allowed to be large enough by parallel interval OFDM transmission. I use the cyclic prefix to remove completely before every OFDM symbol transmitted.

OFDM Transmitter parts are related in Diagram 2.2 showing the way the signal is transmitted. Mathematical formulas demonstrate more details as will be given in the next sections.

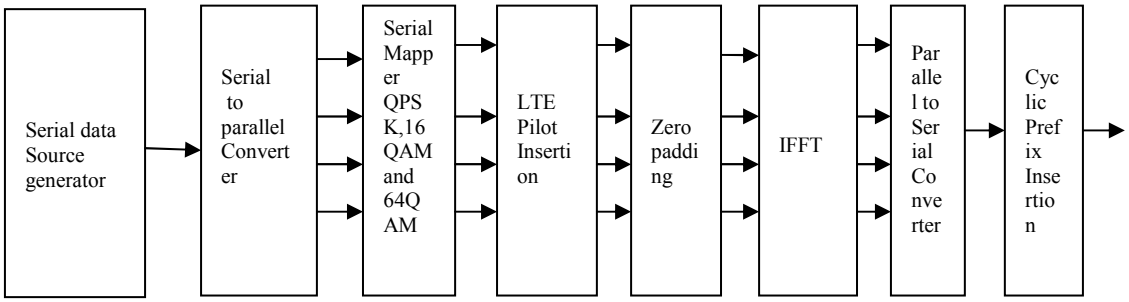

Figure 2.2: Block-Diagram of the OFDM UMTS-LTE transmitter

2.3 Source Generation:

The modeling of the data digital or analog in the communication system is done by a random binary source generator with equi-probable bits.
D = [d0, d1, d2, d3, d4… dn] and d*i* = {0, 1}
The number of generated random integers in the form of bits per symbol and the number of sub-carriers are given by the modulation scheme. The data rate and the efficiency are developed by the constellation.

2.4 Digital Modulation Methods:

QPSK, 16 QAM, and 64 QAM are commonly used modulation schemes. First serial to parallel conversion of data and then mapping are done here. High data rate, bandwidth and capacity for the UMTS-LTE are achieved by 16 QAM and 64QAM which are implemented in the LTE transceiver and QPSK. These are discussed in the following topics:

2.4.1 Quadrature phase-shift keying (QPSK):

This is high order scheme and a pair of every two consecutive bits converted from serial to parallel and mapped to complex constellation in the modulator as shown in fig 2.2 [3]. There are 2 bits/symbol, 4bits/symbol, and 6bits/symbol for QPSK, 16QAm and 64 QAM respectively. The constellation diagram for the modulation scheme or four points with each of two data bits are shown in the figure:

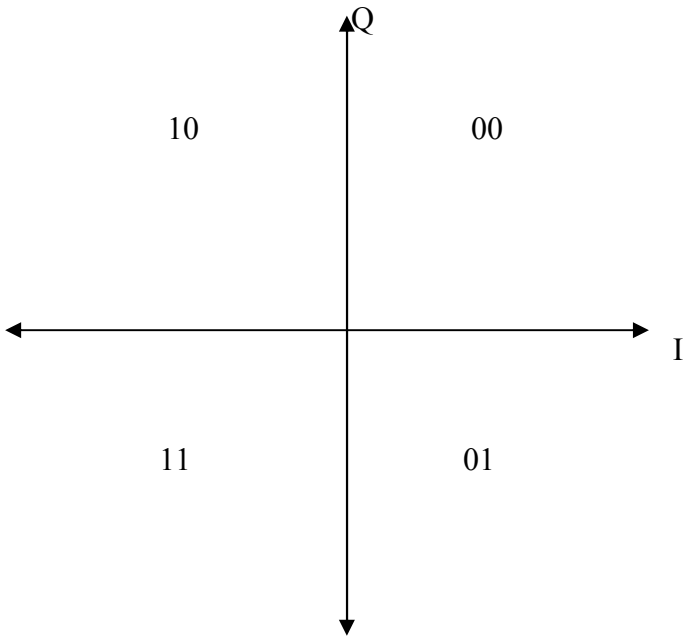

Figure: 2.3 Constellation diagram for QPSK

2.4.2 16-Quadrature Amplitude Modulation (16QAM):

It is an efficient and high data rate, uses 4 bits/symbol. It produces high data rate than QPSK. The 16 QAM constellation figure is given as.

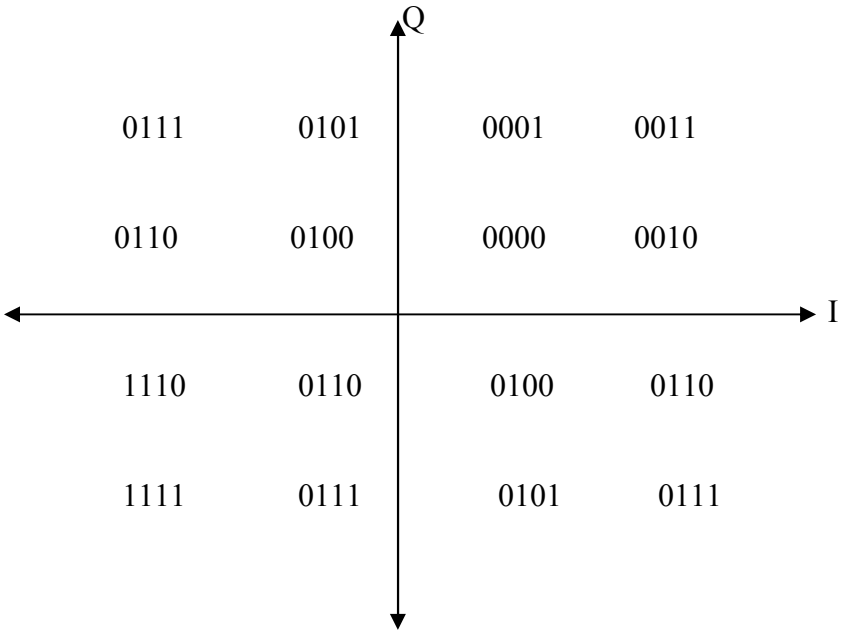

Figure: 2.4 Constellation diagram for 16QAM

2.4.3 64-Quadrature Amplitude Modulation (64QAM):

This is capable to carry an amount of even higher data rate .There are 6bits/symbol mapped and used in the system like 802.11 a/g. As the symbols are equal, normalization of all the transmitted symbols is done. Constellation diagram of 64 QAM is shown similar case applied here as for QPSK and 16 QAM. I have this as shown in fig below.

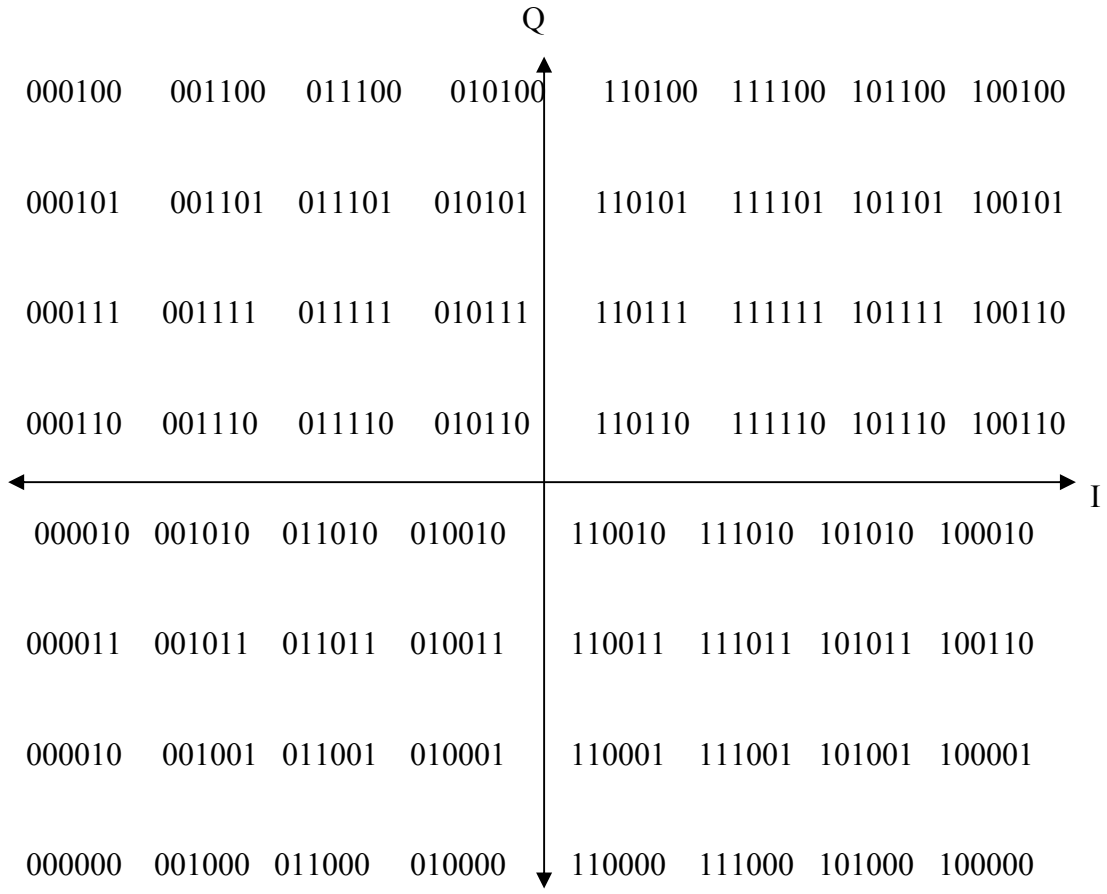

Fig:2.5 64-Quadrature Amplitude Modulation (64QAM)

2.5 UMTS-LTE Pilot Structure:

A frequency selective channel model is used to get UMTS-LTE transceiver system done by simulation process in the multi-path propagation. It is difficult to track and estimate the multi-path propagation in OFDM system. Channel estimation techniques [23,5,18,19, 12] in which pilot symbols are used to various fading channel models and estimation of the instantaneous channel is required to decode the received symbol. The transmitter and receiver with the reference symbols carrying no data in the transmitted signal is done as in standard [1] figure 2.6 provides the downlink reference signal structure symbols to estimate channel. Main uses for this in LTE downlink reference [1] are as:

Frequency Domain

D	**R_1**	D	D	D	D	D	**R_1**	D	D	D	D	D	**R_1**	D	D	D	D	D
D	D	D	D	D	D	D	D	D	D	D	D	D	D	D	D	D	D	D
D	D	D	D	D	D	D	D	D	D	D	D	D	D	D	D	D	D	D
D	D	D	D	D	D	D	D	D	D	D	D	D	D	D	D	D	D	D
D	D	D	D	**R_2**	D	D	D	D	D	**R_2**	D	D	D	D	D	**R_2**	D	D
D	D	D	D	D	D	D	D	D	D	D	D	D	D	D	D	D	D	D
D	D	D	D	D	D	D	D	D	D	D	D	D	D	D	D	D	D	D

Figure: 2.6 Basic downlink reference signal structure

R_1: First Reference symbol
R_2: Second Reference symbol
D: Data
Time period: 0.5 ms

- Measuring the channel quality
- Estimation for different demodulation and detection at the end user side
- Cell search and Initial acquisition

This transmission of pilot symbols is an efficient way of tracking multi-path . By the assumptions of [1, section 7.1.1.1.2.2], neither all the frequencies bits nor the all transmitted OFDM symbols consists of pilots for UMTS-LTE.
Figure above shows the OFDM symbols considered for the implementation with pilot tones.

2.6 Zero Padding, OFDM Modulation, And Cyclic Prefix Insertion:

2.6.1 Zero Padding:

In the simplification of analog filter realization, the sampling rate is greater than bandwidth. That is why I use the zero fading in design at the transmitter. This will increase the spectrum signal length which is not the integer multiple of total length of signal. Length is adjusted by the time band limits or the frequency band limits. The time domain extension with zeros to signal is used. Fig depicts this as shown.

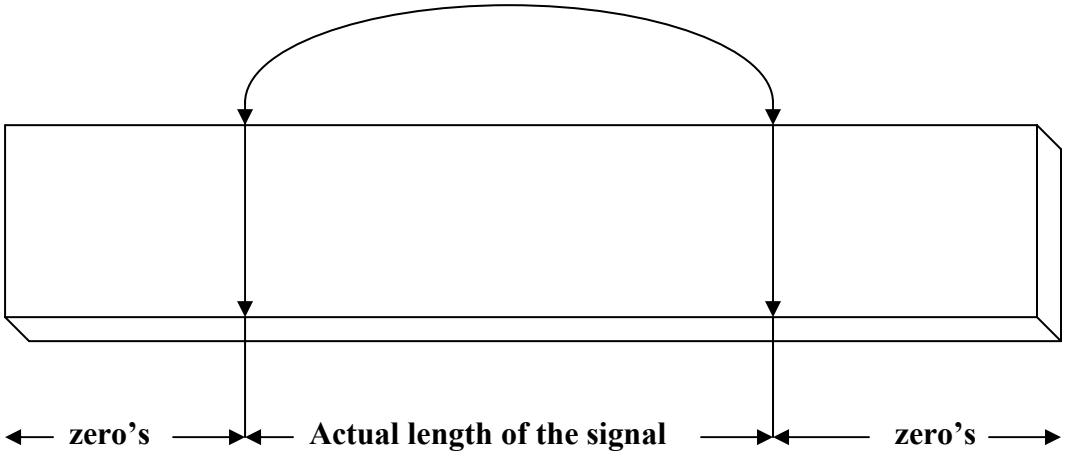

Fig: 2.7 Zero padding in the time domain

2.6.2 OFDM Modulation:

The transmitted data is divided into low bit rate streams on OFDM schemes are carried as sub-carriers [20,23]. So OFDM is an efficient technique and selected by many wire line and wireless application. IFFT will reduce the complexity of the transmitter and I implement OFDM at the receiver part .DFT is required to demodulate the data as the low complexity FFT. Higher data rate is achieved but low rate streams are subjected to individual flat fading as it is transmitted over the selective frequency channel model.

X (1), X (2), X (3), X (4)… X (N)

are the transmitted symbols if Nsc sub-carriers .Mathematical discrete time representation for symbols is given as and is done by the normalization of all the OFDM IFFT symbols. Equation 2.1 showing this as:

$$X(k)=1/\sqrt{N}\sum_{n=0}^{N-1} X(n) \times e^{-2\pi j\,(kn/N)}\, X(k) \qquad (2.1)$$

Where k=0……N-1

The time domain symbols OFDM data are obtained by FFT given by the relation;

$$Y(n)=1/\sqrt{N}\sum_{k=0}^{N-1} y(k)\; e^{-2\pi j\,(kn/N)}\, Y(n)$$

Where n=0…..N-1

2.6.3 Cyclic prefix:

Wireless communication in multi-path faces many problems while the transmission is going on. Interference symbol and inter carrier interference are common over the time varying frequency selective channels. Cyclic prefix reduces the inter symbol interference which is similar to the last part of the transmitted OFDM symbol. Fig 2.8 demonstrates the cyclic prefix. Cyclic prefix must be adapted to delay spread related to signal. Short

and long are the two lengths in UMTS-LTE operation as in [1]. There are some conditions in the length must be same or longer than the channel impulse response length to get rid of interference.

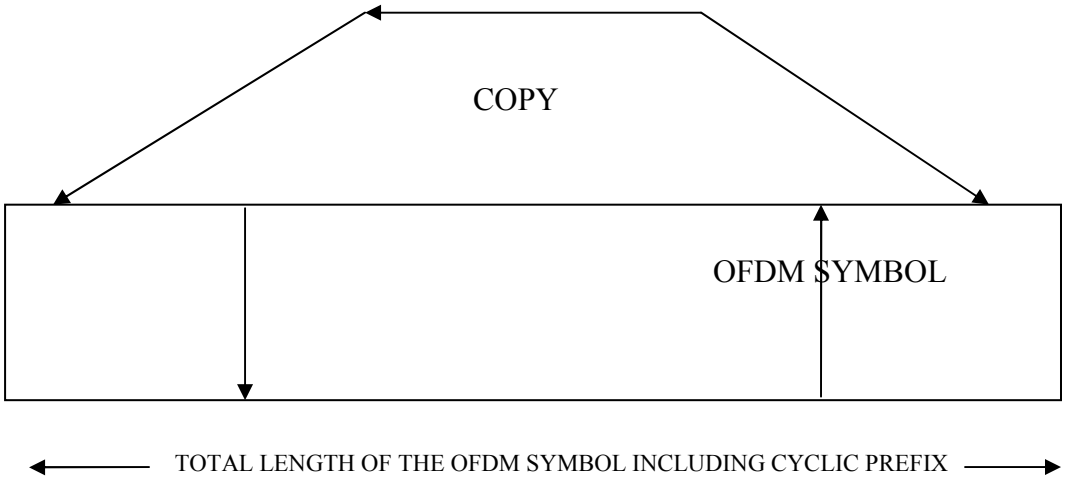

Fig: 2.8 The cyclic prefix addition to the transmitted OFDM symbol

2.7 OFDMA:

The spectrum is divided into multiple sub-carriers which are orthogonal to each other and modulated by the low bit rate streams. OFDM system is developed in downlink transmission for the E-UTRA FDD and TDD modes. The WLAN, WIMAX and the broadcaster technologies like DVB are commonly used in the OFDM. It is robust comparing the multi-path fading form. Fig 4.8 represented an OFDM signal taken from [2]. Select 5MHz and principle remains the same for the E-UTRA. After modulation the transmission over the orthogonally spaced sub-carriers bandwidth is done. QPSK, 16QAM, and 64 QAM are the schemes for E-UTRA. To face inter symbol interference a guard time interval is added to each symbol which is cyclic prefix and is put before OFDM symbol.

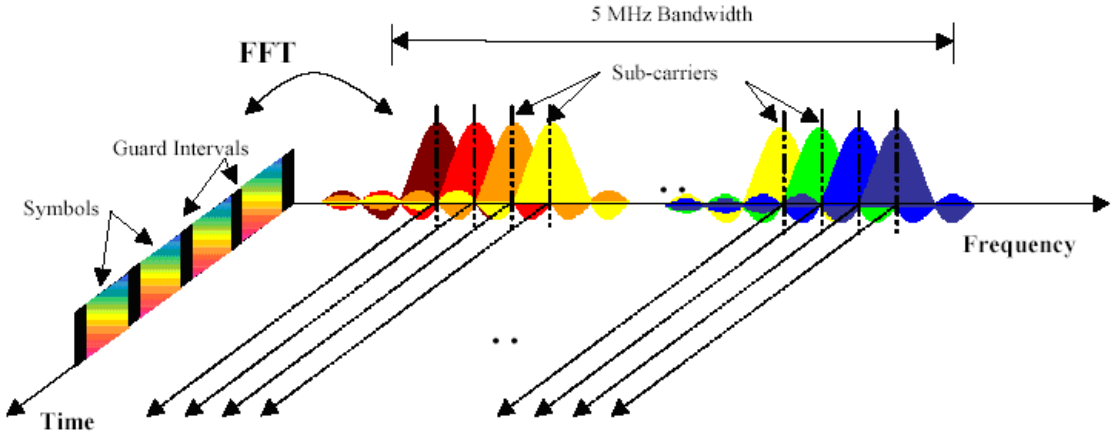

Fig: 2.9 Frequency-Time Representation of an OFDM signal

IFFT generates OFDM as it converts a N number of frequency domain complex symbol into time domain .In the figure below N point IFFT and a (mN+n) as the nth sub-carrier channel modulated data symbol in the time period mTu < t̃(m+l)Tu.

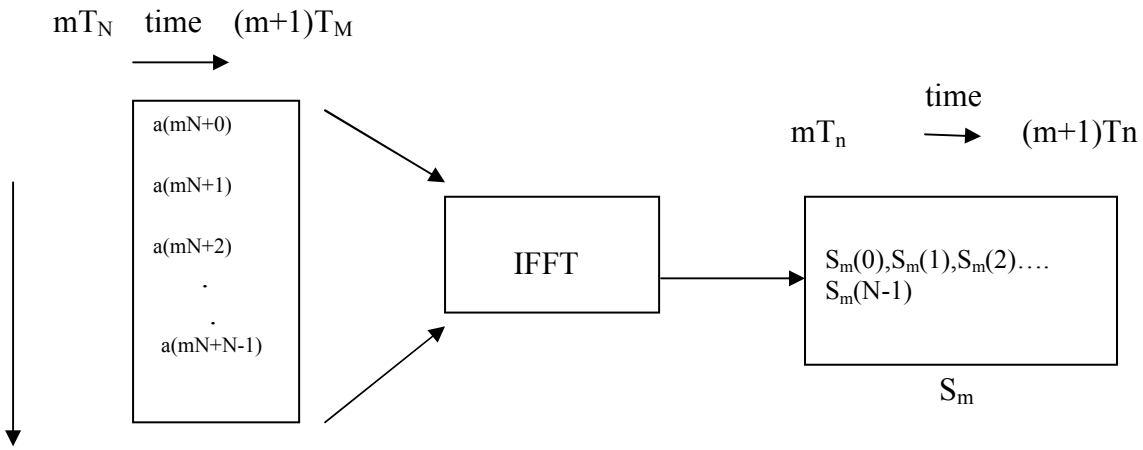

Figure: 2.10 OFDM symbol S_m as superposition of N narrowband modulated

The vector S_m is the OFDM symbol and it is superposition of N narrowband modulated sub-carriers. A parallel stream of N sources modulated data provides a wave form of N orthogonal sub-carriers and sub-carrier shape is frequency Sinc function as in fig. 2.9. In Figure 2.11, mapping is shown as a stream serial of QAM symbols to N parallel streams in the form of frequency domain for the IFFT. Then a time domain signal is obtained by the N-point time domain system.

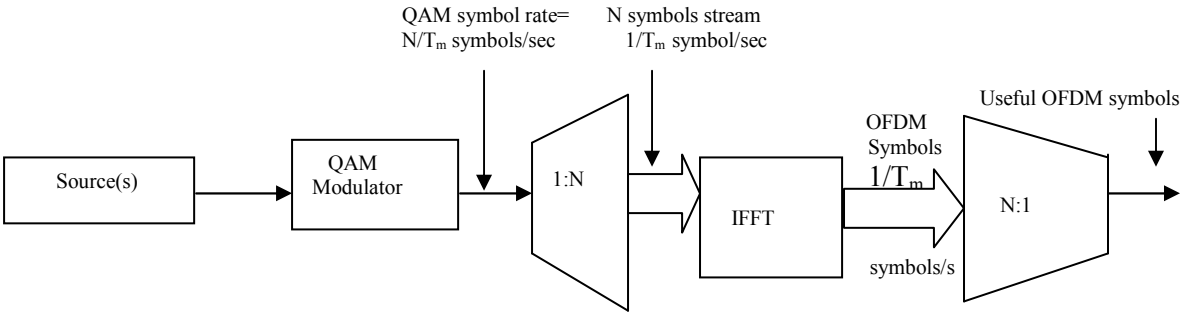

Fig:2.11 OFDM Signal Generation Chain

Multi-path users are allowed in OFDMA as compared to an OFDM scheme. The principle is that the data channels are shared in E-UTRA, is a specific time frequency assigned to each user. Each transmission time interval of 1ms requires new scheduling decision assigned to time/frequency resources.

2.8 Motivation of Receiver Structure:

The UMTS-LTE transceiver and the receiver part is designed for it at the user terminal (UT) side. The specific requirements about the low complexity and low cost should be assured. There are certain constrains of stringent power consumption as the mobile receivers are small. Receiver side has some additional operations with respect to the transmitter side. The signal received is in the form of convolution of the multi-path channel impulse response h(t) and the transmitted signal s(t). The guard period has been removed from the received signal. This is inverse process to the one at transmitter side and it is de-cyclic prefix. Fast Fourier Transform (FFT) converts the transmitted signal into the frequency domain and I obtain the modulated symbol values. In order to deal with the effect of the multi-path channel, a suitable channel-estimator is identified and implemented. As UMTS-LTE is an OFDM based system, the proposed Minimum Mean-Square Error (MMSE) channel-estimator in [80] has been implemented in this design. Here All the received signal sub-carriers experience a complex gain, amplitude and phase distortion, due to the multi-path fading channel. To counteract such influence of the channel, a simple frequency-domain equalizer (FDE), the LMMSE equalizer is employed. Afterwards, soft or hard QAM de-mapping schemes are employed. According to the assumptions made earlier, this system is an un-coded system; however, the coding part has been left as a future work. Further, it is also assumed as a fully synchronized OFDM transceiver system.

The aforementioned UMTS-LTE receiver parts are discussed in more details throughout this chapter. Figure 2.12 shows the different parts of the UMTS-LTE receiver.

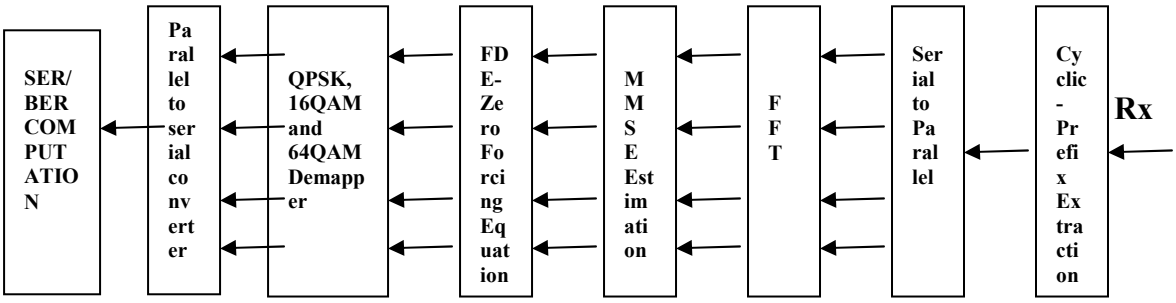

Fig 2.12: Block-Diagram of the OFDM UMTS-LTE Receiver

2.9 OFDM Demodulation:

Multiplication of the data sequence by the channel frequency response plus white Gaussian noise provides the received signal and it is distorted in this way. Multi-path channel converts the time domain signal into parallel symbols and discards the cyclic prefix. As the received signal is comprised of convolution of the multi-path channel impulse response h(t) and the transmitted signal s(t). OFDM transmitted symbol does not affect in the actual transmitted data of every next symbol. The Inter-OFDM symbol interference effect is eradicated by the cyclic prefix extraction.

OFDM de-modulation is completed as the received time domain signal converted to frequency domain by FFT, given in figure 2.13. Equation 2.1 has clearly shown the demodulated all N transmitted sub-carriers of the OFDM signal in the form of output of the N complex QAM symbols. Being the orthogonal system, demodulation is done by the multiplexing it with the same carrier frequency. The process is summed up by the sampling at receiver. Wide band systems use the FFT. Figure 2.13 depicts as DFT transforms from time domain to frequency domain and vise versa.

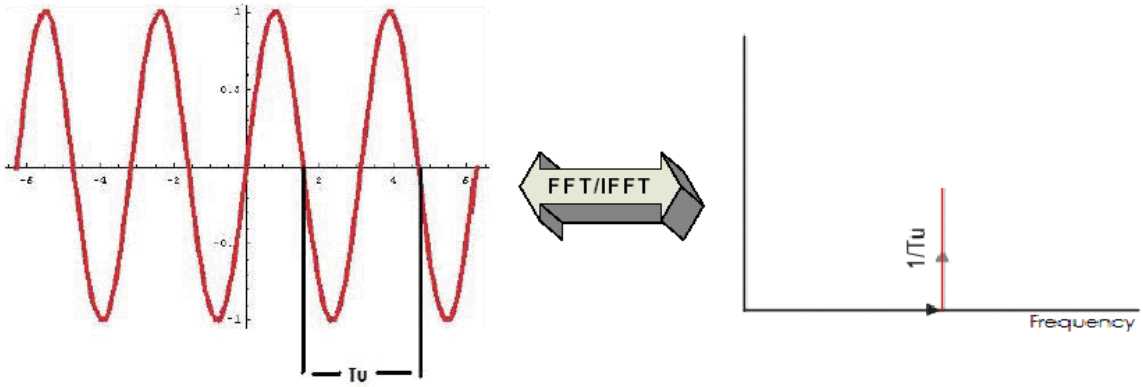

Figure2.13: DFT converting from Time-domain to Frequency-domain and Vice-versa

2.10 Channel Estimation:

The channel estimation technique used to estimate the realization of the multi-path channel effect in the receiver. The multi-path channel effect has problem as the each sub-band is disturbed by a channel of different random phase and amplitude. the challenging problems in wideband receivers is the tracking the effect of the multi-path channel . The cyclic prefix length used is longer than the channel impulse response in order to ensure that no inter OFDM-symbol interference is present. Generally, the multipath channel estimation can be carried out by using either additional pilot symbols into all sub-carriers of the OFDM symbols at instant time intervals, or by appending pilots into every transmitted OFDM symbol [72]. Pilot symbols can be either defined in the time-domain, or as a training sequence in the frequency-domain and these are called pilot symbols, and the latter are called pilot tones respectively. Pilot tones are known to the transmitter and the receiver part. The channel estimation is based on the pilots that transmitted at a certain positions in the time-frequency grid of the OFDM signal. Pilot tones, defined in [73] and used in my design, are transmitted together with the data symbols which make the design of the UMTS-LTE transceiver more robust against the fading effect of the channel. Based on the assumptions of [73] , I here considered the OFDM symbols that contain pilot tones in the implementation of the channel estimator. There are different channel estimators which can exploit the pilot tones frequencies to estimate the effect of the channel. Among these estimators are Least Square (LS), Minimum Mean-Square (MMSE), and Least Mean-Square (LMS). In [74] both Minimum Mean-Square, and Least Square (LS) channel estimators have been presented and implemented over a multipath faded channel. In UMTS-LTE transceiver design I implemented the Minimum

Mean-Square (MMSE) channel estimators, the modified one presented in [74]. The general channel estimator structure [74] is shown in Figure (2.14).

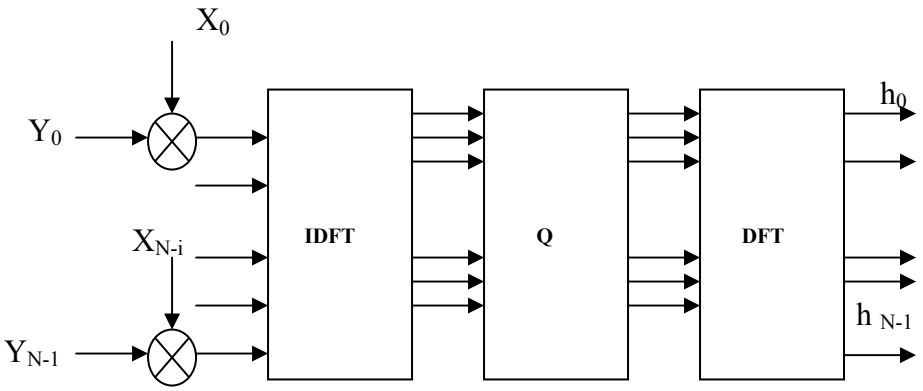

Fig 2.14: General Channel Estimator Structure

The proposed MMSE channel estimator in [74] is providing high performance than the general form. It also shows better performance than the other proposed (LS). Further, to achieve low-complexity and better performance to the UMTS-LTE transceiver system, the modified version of the MMSE estimator, as in [74] has been selected for this OFDM transceiver design and implemented too. Figure 2.15 below shows the modified MMSE channel estimator.

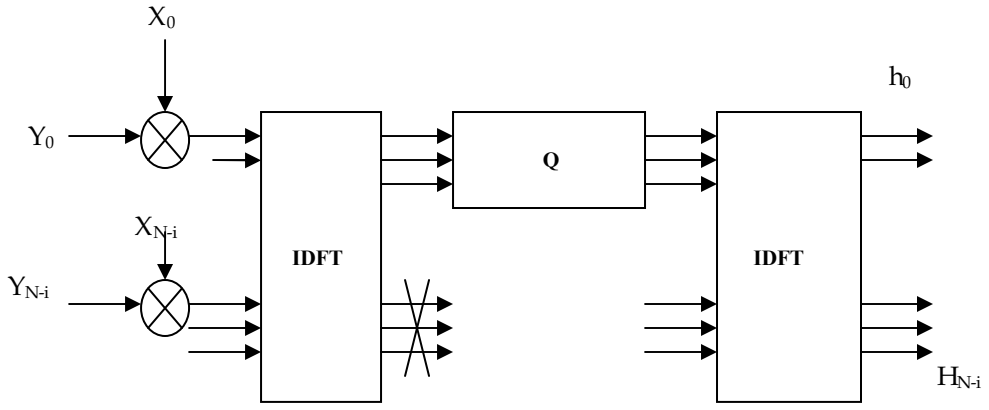

Fig: 2.15 Modified MMSE Estimator Structure

2.11 LMMSE Channel Equalization:

The multiplication of the OFDM signal spectrum in the frequency-domain is caused by the time-domain convolution over the multi-path channel. As a result of this there will be appearance of multiplicative complex channel coefficients on each sub-carrier. Therefore the received sub-carriers will have a distortion on their amplitudes and shift to their

phases due to the multi-path channel effect. I implement a frequency-domain equalizer (FDE) to cope with the multiplicative effect introduced by the multi-path channel. The Frequency-domain equalizers are normally much simpler than their time-domain counterparts and will lead to a low complexity design for the receiver part. The transmitted signal is split up into many streams in OFDM systems. There will be a flat fading in after multi-path channel. As refer to the received signal by Y(n), for sub-carrier n, H(n) is the channel response, X(n) is the frequency-domain transmitted symbol, and N(n) is the additive noise. So I have:

$$Y(n) = X(n) * H(n) + N(n) \quad (2.2)$$

Initially, LMMSE channel estimation is performed on the received signal and then the frequency-domain equalization is performed for each sub-carrier using the estimated channel.

2.12 Frequency Selective Fading Channel Model:

There are several paths in the mobile communication world which are followed by signal from the source to destination. These are distributed as the buildings, vehicles and other obstacles in the way can reflect and cause scattering of signal. So there are many paths between BS base station and UT user terminal for the communication and received is summed as in Figure3.2. The paths have frequency response as superposition in this domain with a different Doppler shift and attenuation. the received signals from the paths will add up at the terminal side . Its power may vary depending on the distribution of the carrier phases and constructive or destructive values. There may be two fading due to fluctuations involved as Rayleigh fading in case of power varying randomly. The frequency selective fading is caused by different frequency domain at a point in the multi-path propagation. this result when there is multi-path phenomena as the transmitted arrives at the receiver with different spreading. As the length of the delay spread time is less than the period, or the bandwidth is less than the coherence bandwidth, all the frequencies face flat fading at the point. In case the length of delay spread is greater than the symbol period, or the signal bandwidth is higher than the coherence, the channel is selective fading channel model as given here:

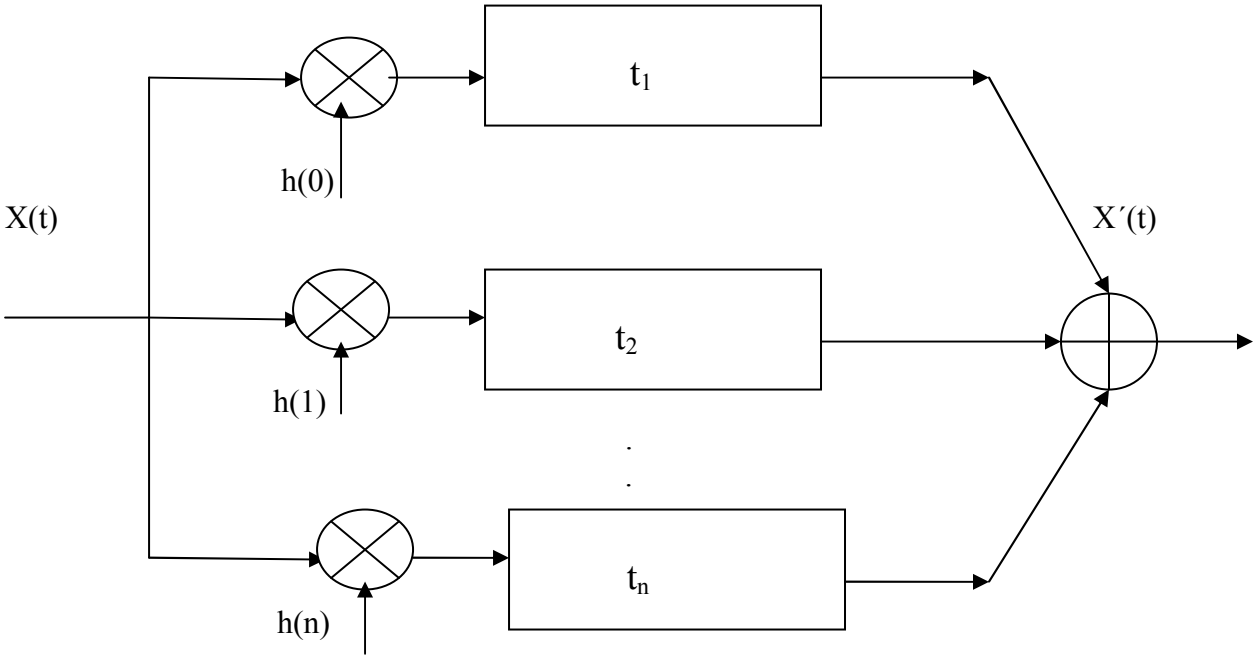

Fig2.16: Frequency selective channel model

The fig indicates as the transmitted signal is divided into many frequencies and each is experiencing a different effect in this frequency selective fading channel model.

2.13 ITU channel models:

Time variant channels A and B for the vehicular and pedestrian are used for designing the UMTS-LTE transceiver in particular selective frequency. Modes are chosen for the requirements of the new LTE technology of the mobile generation. These are very efficient for the design because I need the higher robustness of the communication system. Pedestrian and vehicular are the categories in the models. There are two in pedestrian as A at 3km/h, (PA3) and B at 3km/h (PB3) and three in vehicular as A at 30 km/h (VA30), A at 120 km/h (VA120), and A at 350km/h (VA350). The high speed trains are obtained in 3GPP by 350 km/h.

There are different delay taps number representing delay and power of the signal path. Channel power delay profiles are suitable for explaining the propagation. The Tables [21] describes the power profiles as given.

1. ITU pedestrian A (PA3) gives relative delay and the relative mean power as in table:

Relative Delay [ns]	0	110	190	410
Relative Mean Power [dB]	0	-9.7	-19.2	-22.8

Table2.1: ITU Pedestrian A channel model

2 ITU Pedestrian-B (“PB3”) gives Relative delay and power profiles for this channel as in table :

Relative Delay [ns]	0	200	800	1200	2300	3700
Relative Mean Power [dB]	0	-0.9	-4.9	-8.0	-7.8	-23.9

Table2.2: ITU Pedestrian-B Channel model

3 ITU Vehicular-A (“VA30”), (“VA120”), and (“VA350”) give Relative delay and power profiles for these channels as in table:

Relative Delay [ns]	0	310	710	1090	1730	2510
Relative Mean Power [dB]	0	-1.0	-9.0	-10.0	-15.0	-20.0

Table2.3: ITU Pedestrian A channel models

2.14 Doppler shift:

As there are many different paths with electromagnetic propagation and different Doppler shift is exhibited in each path which is resulted due to the relative motion of the transmitter or receiver with respect to each other. The frequency components are affected and frequency shift occurs and Doppler shift is calculated by the equation.

$f_{d=}(f_c x v / c) \times \cos\alpha$

From equation, $\mathbf{f_d}$ is the Doppler shift, $\mathbf{f_c}$ is the carrier frequency, **v** is the speed of the antenna, **c** is the velocity of light, and **á** is the angle of arrival of the received signal. when the direction is opposite between the antennas, then the maximum Doppler shift as calculated by the relation as:

$f_{d\,max} = (f_c x v)/ c$

2.15 Delay spread:

The transmitted signal copies received at the receiver side are different because the time difference between first and last one. This maximum time difference between first echo and the last path is called the delay spread. Flat fading in case if the length of spread is less than the symbol period and the channel is frequency selective if the delay spread higher than the symbol period.

2.16 Soft and Hard De-mapping

Mapping schemes improve the spectral efficiency and increase the bit rate. QAM is defined in [1] and performs mapping of the bits at the transmitter part. Certain operations are necessary to be done at the receiver part. Hard de-mapping is used here and soft de-mapping is determined by long likelihood ratios (LLR).
Fig 2.16 describes the QAM de-mapping .

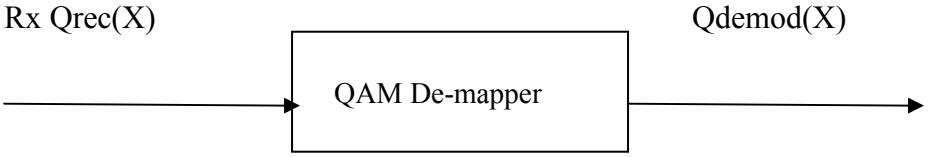

Fig 2.17:The QAM De-mapping block diagram

Equation 2.3 given below actually determines the LLR operation. Qrec (x) and bit by bit probability estimation is measured by it. Z represents the corresponding bits before de-mapping as in figure 2.23.

$$\lambda(Q_{rec}(X))= \log(pr\{Q_{rec}(x) =+1|Z\}/Pr\{Q_{rec}(x)=-1|Z\}) \quad (2.3)$$

The soft detection of QAM is done by the LLR bit by bit processing and the LLR has a definite range [-8,8].

2.16.1 Quadrature phase-shift keying (QPSK):

The de-mapping to bits of received symbols is done. The hard de-mapping for the QPSK is completed by the function of it . In a way to split the received equalized signal into two parts. Each of these in-phase and Quadrature carriers de-mapped, the original boundary signal is reconstructed by a two multiplexed out put stream.

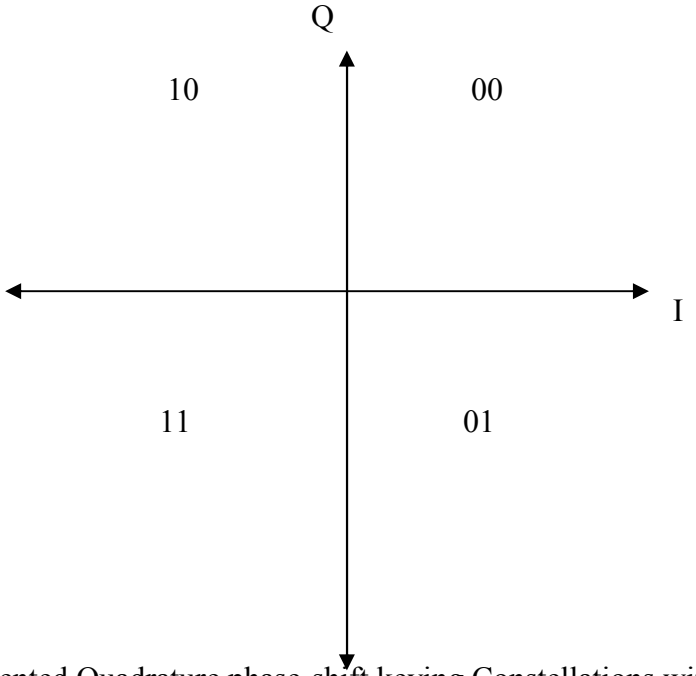

Figure2.18: Implemented Quadrature phase-shift keying Constellations with Gray-Mapping

2.16.2 16-Quadrature Amplitude Modulation (16QAM):

In this technique the in phase and quadrature components are demodulated separately and soft and hard de-mapping are used. Two streams are de-mapped by 4 Amplitude Phase Shift Keying in phase and 4 ASK Quadrature carriers in hard de-mapping. In case of soft de-mapping LLR ratios are used.

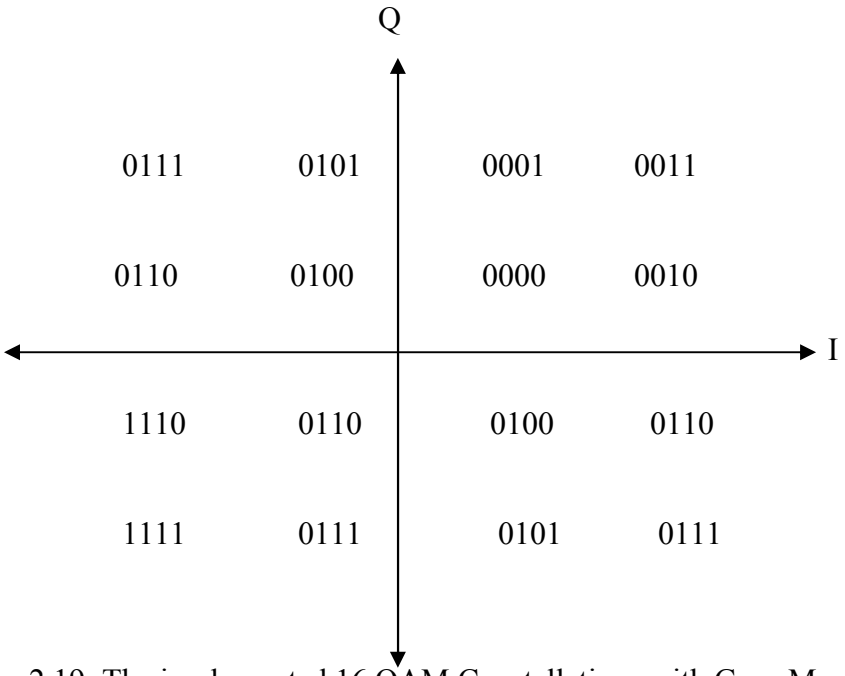

Figure2.19: The implemented 16 QAM Constellations with Gray-Mapping

2.16.3 64-Quadrature Amplitude Modulation (64QAM):

This is implemented as the two bit stream de-mapped by 8ASK for in-phase and Quadrature carriers. The bits in every OFDM symbol with other symbols are considered. 16QAM [3] and 64QAM [6] are the gray coding schemes used at the transmitter and receiver part respectively. These are shown in fig 2.18, 2.19 and fig 2.20 indicate the LLR on 16QAM constellation symbol.

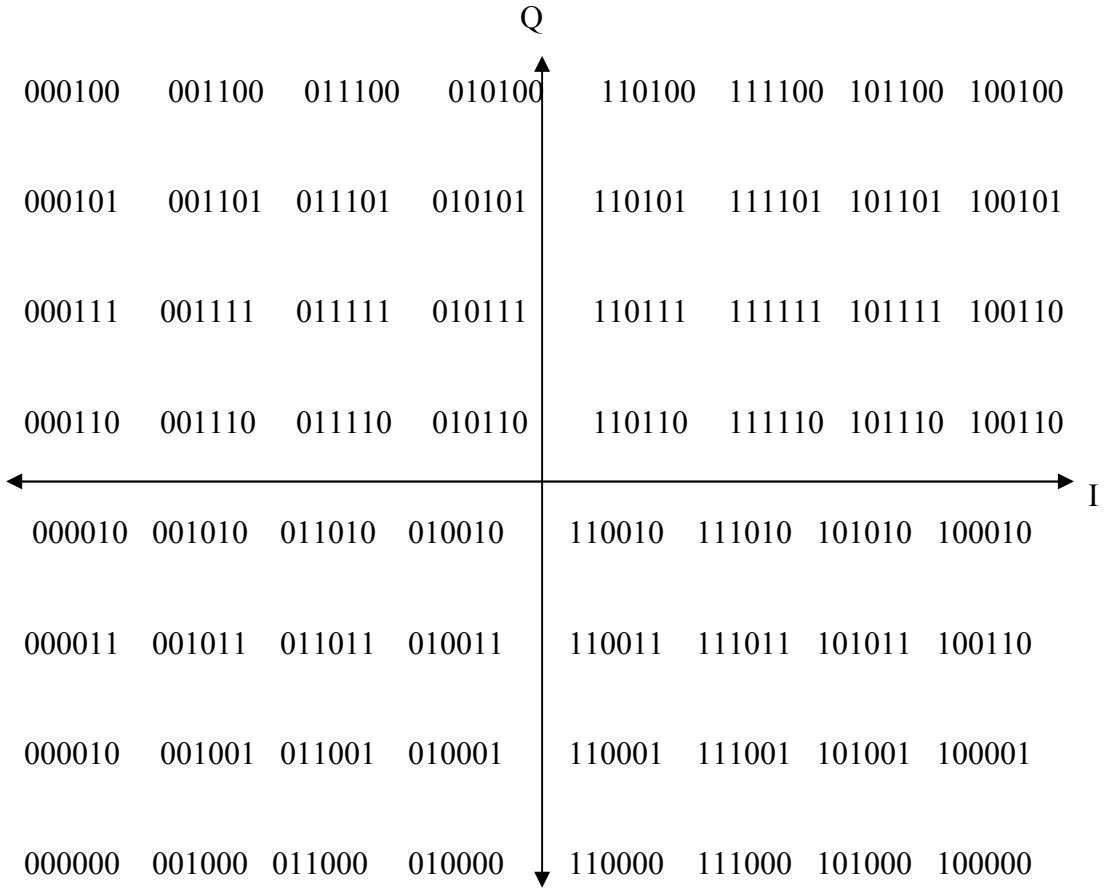

Fig2.20: The implemented 64 QAM constellations with Gray-Mapping

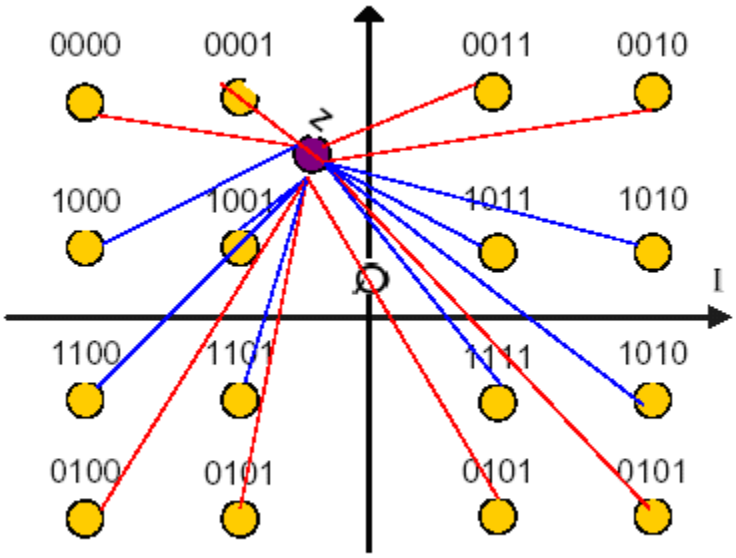

Fig2.21: LLR on the 16QAM constellation symbols

2.17 LTE Uplink Transmission Scheme:

2.17.1 SC-FDMA:

Alternative investigation for the optimum uplink was performed in the LTE study. OFDM fulfills the requirements of LTE in downlink but it is not suitable for uplink because of having weaker peak to average power ratios (PAPR). That is why SC-FDMA with cyclic prefix is used for FDD and TDD in LTE uplink. These PAPR characteristics are better to get cost effective testing of UE power amplifier. As there are some similarities the parameterization of uplink and downlink can be harmonious. DFT spreads OFDM for E-URTRA and it is selected to generate an SC-FDMA signal as in fig 2.21.
M-size DFT is applied to a block of M-modulation symbols. QPSK, 16QAM and 64QAM are the main techniques for the uplink E-UTRA schemes. Mapping for the sub carriers is available here. Transformation of the modulation symbols into frequency domain is done by the DFT. Only localized transmission on consecutive sub-carriers is allowed as N point IFFT (M<N) as in OFDM following the cyclic prefix and parallel to serial.

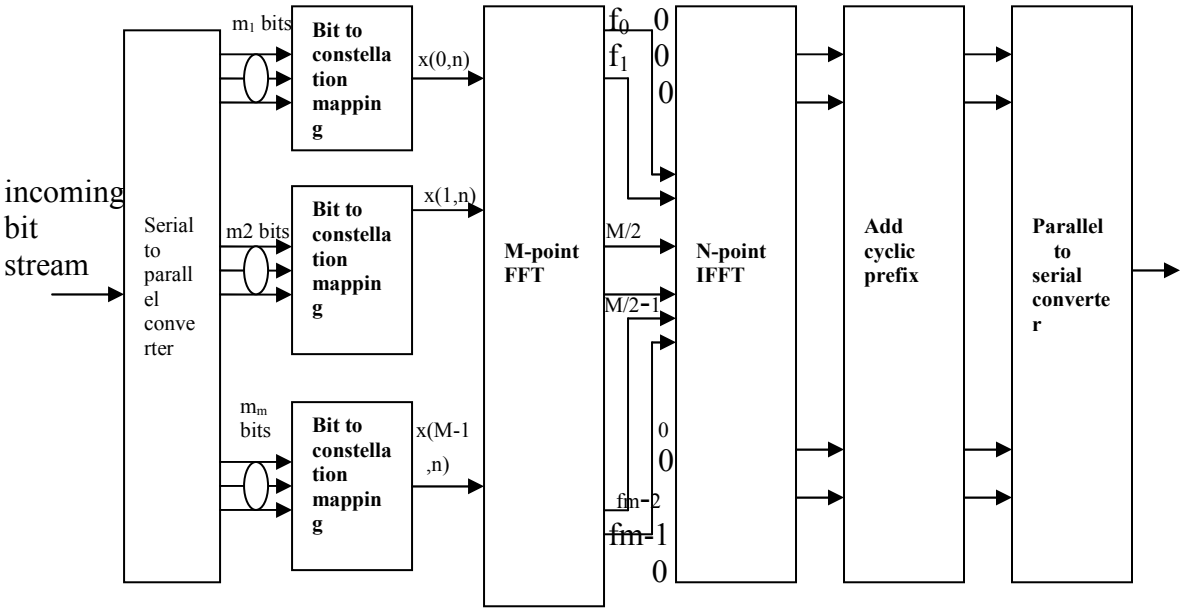

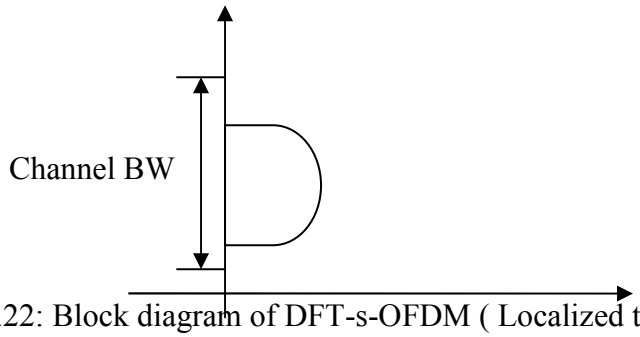

Fig2.22: Block diagram of DFT-s-OFDM (Localized transmission)

DFT-spread-OFDM is simple difference between SC-FDMA and OFDMA signal generation. Information about all the symbols of transmitted modulation have been spread over the sub carriers by the DFT while OFDMA signal carriers information are related to modulation symbols.

2.17.2 SC-FDMA Parameterization:

Downlink structure is similar to E-UTRA uplink with 20 slots of 0.5 ms and each sub frame of 2 slots as shown . Slot carries uplink symbols as N SC-FDMA symbols (N=7 for normal cyclic prefix and N=6 FOR extended cyclic prefix). The fourth symbol in the slot carries reference signal for channel demodulation.

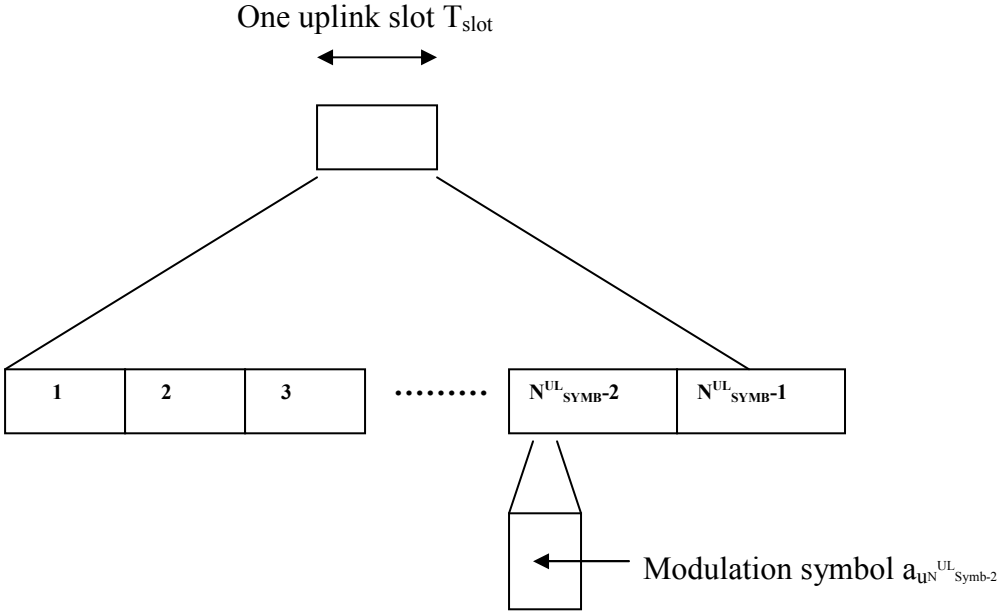

Fig2.23: Uplink slot structure

A bandwidth agnostic layer 1 specification for uplink has been selected.

Configuration	Number of symbols	Cyclic prefix length in samples	Cyclic prefix length in μs
Normal cyclic prefix Δf= 15 KHz	7	160 for first symbol 144 for other symbols	5.2 μs for first symbol l 4.7 μs for other symbols
Extended cyclic prefix Δf= 15 kHz	6	512	16.7 μs

Table2.4: Parameters for uplink generic frame structure.

2.17.3 Uplink Data Transmission:

There is a same uplink resource block size as the downlink in the 12 sub-carriers frequency domain. The factors 2,3 and 5 are allowed in uplink to simplify DFT and transmission time interval is 1 ms. Physical Uplink Shared Channel (PUSCH) data is determined by the transmission band with NTx and the frequency hopping pattern K0. It carries uplink information for example CQI and ACK/NACK which is same as data packets in downlink. This is transmitted on reserved frequency region.

2.17.4 Uplink Reference Signal Structure:

Two different purposes of uplink reference, one is used for channel estimation in the eNode B receiver to demodulate control and data channels, second provides channel quality in the base station as a basis for the scheduling decisions. I have the sequence for the uplink reference signals as CAZAC (Constant Amplitude Zero Auto-Correlation) sequences.

2.17.5 Uplink Physical Layer Procedures:

This is especially very important in E-UTRA.

2.17.5.1 Non-synchronized random access:

In the transmission from idle-to-connected or to establish uplink synchronization, the random process may be used to request initial access.
Fig. shows this structure as:

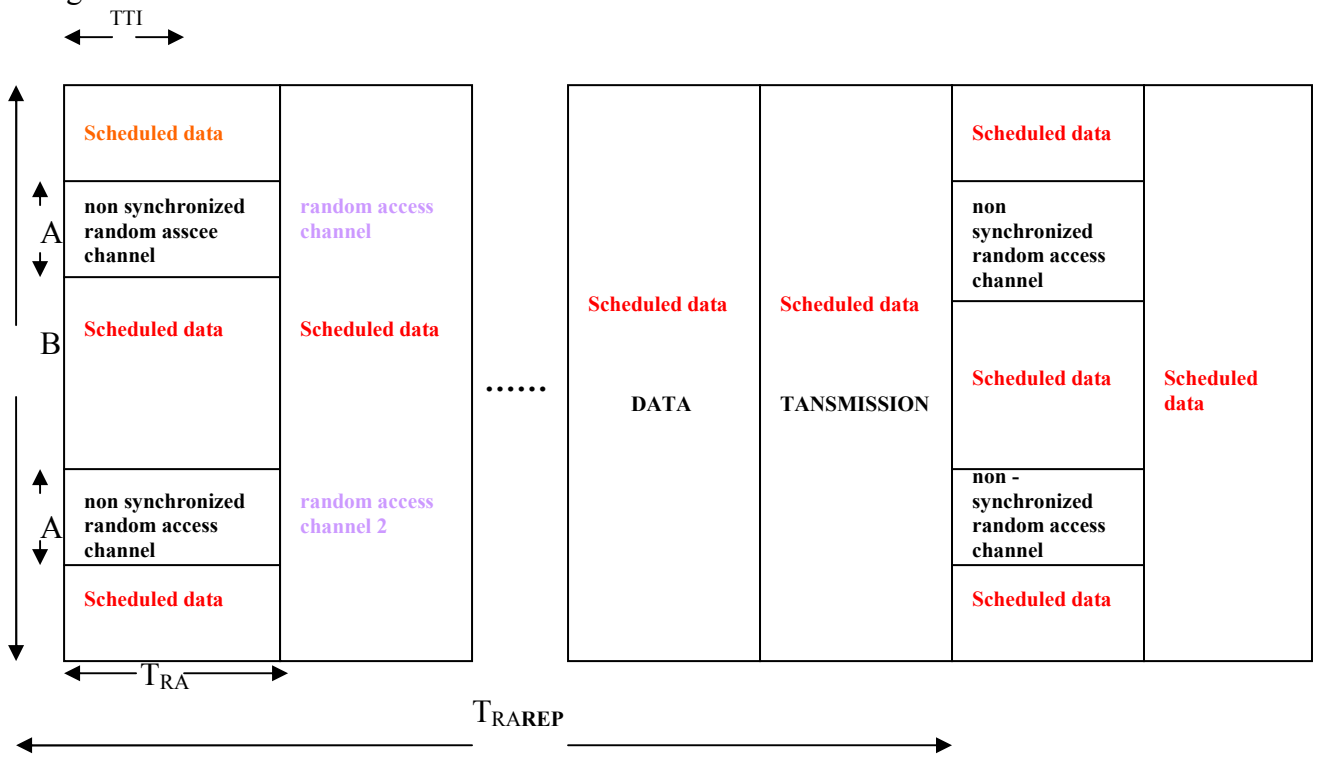

$A=BW_{RA}$, $B=BW_{SYSTEM}$

Fig2.24: Random access structure

This can be defined in frequency domain to provide sufficient number of random access opportunities. Fig: 2.25 has a preamble .It occupies TPRE=0.8ms and cyclic prefix occupies TCP=0.1ms in a sub frame of I ms. Transmission depends on on guard time. Bandwidth of preamble=1.08 MHz(72 sub-carriers) when the transmission is allowed as the higher signaling controls. 64 random access preambles in each cell are created by Zadoff-Chu sequences.

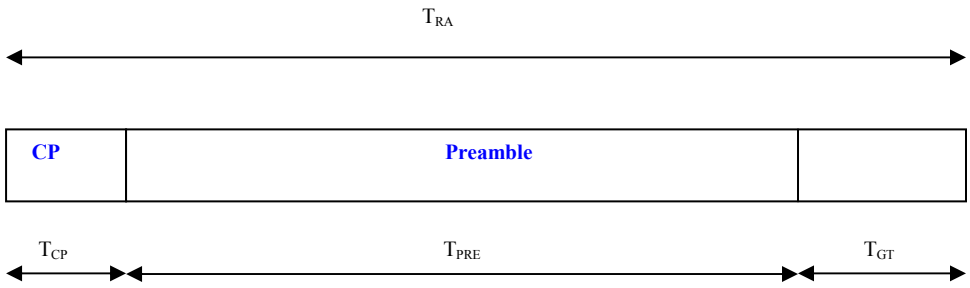

Fig2.25: Random access preamble

Power ramping similar to WCDMA is used in random process. As the preambles are sent, the UE waits for the response message. In case no response detected this process is repeated again.

2.18 Uplink scheduling:

The e NodeB assigns time/frequency resources to UEs to inform about the transmissions. PDCCH in downlink communicates scheduling decisions affecting uplink to UEs. UE buffer status, UE capabilities, QoS, uplink channel, UE quality measure, UE measurement gaps etc. are the basis.

2.19 Uplink adaptation:

There are certain things considered as the transmission power control, adaptive modulation, channel coding rate and adaptive bandwidth.

2.20 Uplink timing control:

It is essential to control to give the transmission from different UEs with receiver of e NodeB. It sends the timing control as UEs in downlink to adopt the respective timing of transmit.

2.21 Hybrid ARQ:

In this case e NodeB requests the transmissions of data packets.

2.22 Channel Model Motivation:

In efficient wireless communication the propagation of the radio frequencies is carried out through communication channels. There are certain channels as the Additive White Gaussian Noise channel model (AWGN), and the frequency-selective channel model. I use AWGN channel here even though the LTE channel model is fading. The (AWGN) channel model investigates the effects of real channels on the performance of communications systems and easy to implement with the available computer simulation tools as Matlab which is one of the tools that used in simulating such models. Both AWGN and Frequency selective channel model are used to simulate and test the feasibility of the UMTS-LTE transceiver.

Chapter 3 System Model

3.1 The MIMO model:

Consider the linear MIMO system as shown in figure 3.1 to communicate over the channel. I have to find the detection of a set of M transmitted symbols from a set of N observed signals. The non-ideal communication channel disturbs observations due to an additive noise vector as shown:

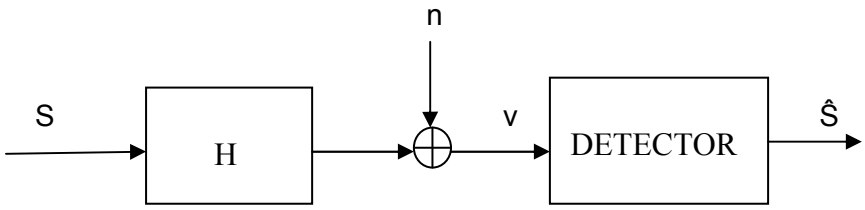

Fig:3.1 MIMO Communication System Diagram

The simplified linear MIMO communication system diagram is showing the discrete time signals transmitted symbols vector $s \in X^M$, channel matrix $H \in R^{NXM}$, additive noise vector $n \in R^N$, received vector $v \in R^N$, and detected symbol vector $\hat{S} \in R^M$.

3.1.1 Transmitted symbol vector:

Finite alphabet $X = \{x_2,..... x_B\}$ of size B indicates the transmitted symbols to get the goal. The B possible transmitted symbol vectors, $s \in X^M$ are selected based on the available data.

3.1.2 Detected symbol vector:

As a result an optimal detector should returns as $\hat{S} = S_*$, given the observed signal vector v, is the largest the symbol vector and its posterior probability of having been sent as:

$$s_* = \text{argmax } s \in X_M \, P(s \text{ was sent } | \text{ v is observed } |) \qquad (3.1)$$

Equation (3.1) is called as the Maximum A posterior Probability (MAP) detection rule. Suppose the symbol vectors $s \in X^M$ are equi-probable that P (s was sent) is constant then the optimal MAP detection rule can be :

$$s_* = \text{argmax } s \in X^M \, P(v \text{ is observed } | s \text{ was sent}) \qquad (3.2)$$

Maximum Likelihood (ML) detector always returns an optimal solution to satisfy (3.2). The additive white Gaussian noise n is considered to express the ML detection problem of Fig. 3.3 as the minimization of the squared Euclidean distance metric in order to meet a vector v over an M-dimensional finite discrete search set as:

$$s_* = \text{argmin } s \in x^M |v - Hs|^2 \quad (3.3)$$

The optimization variables s and $|v - Hs|^2$ as the objective function are measured from the optimization literature. The wireless communication problems examples can be explained by defining the channel matrix H, the ML detection of lattice coded signals, QAM-modulated signals transmitted over MIMO at fading channels and frequency selective fading channels, as well as multi-user channels.

3.1.3 Channel Matrix Preprocessing

The symbol decisions in the tree search are implicitly supposed such as starting from the last symbol in $\hat{s}$, as s_m. For an arbitrary permutation matrix, $\pi \in R^{m \times m}$, the optimization problem is:

$$\min_{\hat{s} \in Sm} ||y - H\pi\hat{s}||^2 \quad (3.4)$$

as equivalent to the original ML detection problem in (1.4). if ś is the minimizer of (3.4), then $\hat{s}_{ML} = \pi^{-1}$ś. Applying sphere decoder with Hπ as the channel matrix yields an alternative detection ordering given by π. The QR factorization on Hπ is applied such that QR = Hπ, the effective upper triangular matrix R depends on the choice of π. The permuting concept the columns of H by right side multiplication by π will be referred to as channel matrix pre-processing [20] or detection ordering. There is a detection ordering different with respect to the search ordering discussed above. The strategy for the detection ordering and the search ordering can be applied independently.

The choice of π should be such that reduces the complexity of the decoder, or the number of nodes in the search tree. It is shown in [59] that the optimal (in the way that the number of searched nodes is minimized) detection order π must be a function of the channel matrix H and the vector of received values, y. This optimal detection ordering, π, does not look to be tractable.

There are a few suggestions for detection orderings which take the channel matrix, H, and the vector of received signals, y, into account [60, 59]. However, the detection ordering can only be based on channel complexity. An advantage is that the channel matrix pre-processing has to be done once as dealing with the constant deterministic channel or the channel matrix remains constant for many realization of y, a situation is faced when detecting symbols transmitted over the slowly fading channel [20, 3].

It is beneficial to make the admissible range for any intermediate symbol, $\hat{s}_i$, as small as possible. The greatest benefit of this strategy is achieved if the search tree is pruned near the root node at a great extent which corresponds to attempting to maximize the diagonal elements close to the lower right corner of R. A simple strategy is the column norm ordering [20] which sorts out the column of H in the increasing order of their Euclidean norm. There is only limited effectiveness in it as it does not take angle between the columns into consideration and parallel columns may result in a small value along the diagonal R. An effective approach to maximize the minimum diagonal elements of R as the V-BLAST Optimal ordering [61, 20] is used and the results in an ordering can be efficiently computed [6, 62].

3.1.4 AWGN Channel Model:

It is simple and comes from the impairment with this wireless model and the white noise. This noise is characterized by a random signal of certain spectral density and it is obtained by independent random samples from a Gaussian distributions. AWGN does not include any fading, dispersion or interference and a mathematical mode to represent the effect of thermal noise. It consists of a simple wireless channel and is used widely. As shown in the figure the complete picture of transmitter, receiver and AWGN channel. It was initially used for the purpose of confirming the feasibility of the UMTS-LTE.

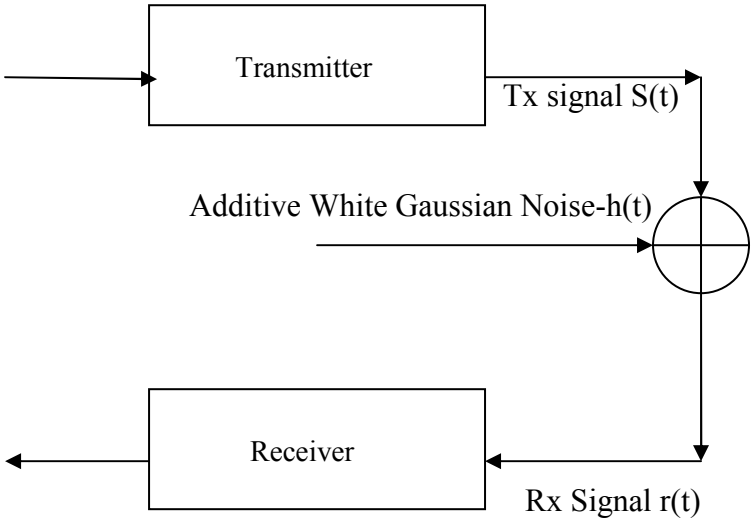

Fig3.2: AWGN channel model

The time difference between the signal echo and last one as the signal received at different instants is called the delay spread. A flat fading results if the spread length is less than the symbol period. Otherwise if greater, the channel is frequency selective.

Chapter 4 Sphere detection

The detection of a vector of symbols transmitted over nxm MIMO channel is discussed in the thesis, where m and n denote the number of inputs and outputs respectively. The input and output relationship of the MIMO channel is given below:

$$y = Hs+v \tag{4.00}$$

where $s \in S^m$ is the finite set of transmitted vector symbols , $y \in F^n$ is the received signal vertor, $H \in F^{nxm}$ is the channel matrix and $v \in F^n$ is the additive white Gaussian noise. Here F is the set of real or complex numbers, i.e. $F \in \{R,C\}$,according to the context. Detection of the vector symbols transmitted over the system channel model according to (4.00) is based upon y and H. A finite set of linearly modulated symbols transmitted over a known linear channel subject to Gaussian noise is modeled on the basis of (4.00) [11, 12]. Properties of receiver algorithms basically focuses on the detection is important here. In the most general term, a detector or receiver refers to a mapping which takes the vector of received signals, y and the channel matrix, H as inputs and thus produces an estimated symbol vector, ŝ as output [11]. That is, a detector is defined by some (possibly random) map.

$$\Phi: F^n F^{nxm} \rightarrow s^m \tag{4.01}$$

where $\hat{s}=\Phi$ (y, H) and F is R or C. Computation of Φ relates to the implementation of the detector. Naturally, the exact interpretation how the detectors are beneficial in this system is debatable. The possibility that the minimum probability of error provided by the receiver in case of transmitted messages $s \in S^m$, is the maximum-likelihood (ML) receiver [14,54], expressed as:

$$\hat{s}_{ML} = \arg \min_{s \in S^m} ||y - H\hat{s}||^2 \tag{4.02}$$

The detector and receiver are always are interchangeable and referred to same thing. The number of symbols m is large enough and results are computationally difficult. A recent review of many possible extensions and improvements over the original algorithm is also provided in [21] under a unified framework which contains virtually all previously proposed implementations as special cases. The algorithm has also been studied under many different communications scenarios. Example include [48] focuses on the multiple antenna channel, [49,50].The sphere decoding (SD) algorithm is for multiple-input multiple-output (MIMO) orthogonal frequency division multiplexing (OFDM) systems.

Sphere decoding which was introduced originally by Finke and Pohst in [7] in 1985, enumerates all lattice points [22] in a sphere centered at a given vector. This detection technique was first applied to the ML detection problem (as it appears in the

communications context in the beginning 90 ’s [18,19,47],which gained main stream recognition with a later series of papers [49,50].The principle of the Sphere Detection algorithm [43,44] is to find the closest lattice point [45,46] to the received signal within a sphere of radius. Hence, it is possible to reduce the computational complexity, by restricting the search area. The choice of is very crucial to the speed of the algorithm where as in practice, it can be adjusted according to the noise (and eventually the fading) variance. The sphere decoder is developed on two stages. Firstly a pre processing stage computes the QR factorization of the channel matrix, H and after this a search stage finds the estimate, $\hat{s}_{ML}$ This detection algorithm has also been observed under many different communications scenarios. Focusing on the multiple antenna channel, with focus on the CDMA scenario, and to generate soft information required by concatenated coding schemes are the examples of different communication scenarios. The sphere decoding algorithm can be illustrated as a tree search procedure by a pruning criteria to reduce the search. It is also notable that there is no possibility that the Sphere decoding estimation does not belong to the set of leaf nodes visited by the algorithm (assuming there are some leaf nodes visited). This decoding algorithm [7] performs a depth-first search over the tree by visiting child nodes before sibling nodes. If the distance exceeds a certain radius d, it falls outside the sphere and is automatically pruned along with its children and siblings (if the latter are enumerated). The radius is updated as the distance to that leaf, if a leaf inside the sphere of radius d is reached. The sphere decoding algorithm also [13] depends on the initial search radius. There will be too many lattice points in the sphere if the initial search radius is too large where as there will be no points in the sphere if the radius is too small. A MIMO channel detector which produces a set of symbols $s \in S^m$ given a set of signals $v \in F^N$ observed at the output of the communication channel, is typically modeled as a linear system $H \in F^{nxm}$ combined with an additive noise vector $n \in F^n$ .I surmise that $M \leq N$ and that H is of full rank M, i.e., there are at least as many observations as symbols to be detected. In the tree search analogy, the sequence of symbol decisions, $\{\hat{s}_{m-k+1} ...,\hat{s}_m\}$ which corresponds to a node of the search tree at the k^{th} level, starts counting from the root of the tree which by default is at the 0 level.The nodes ordering before and during the tree search is important for the algorithm. With appropriate ordering, SD can improve detection performance significantly and provide the number of nodes required to search or the required number of multiplications to achieve maximum likelihood detection performance.

4.1 Sphere decoding fundamentals:

The sphere decoding is based on the enumeration of points in the search set which are found within the sphere of some radius centred at a target such as the received signal point. The Fincke-Pohst (F-P) and Schnorr-Euchner (S-E) techniques are the two computationally efficient means of realizing this enumeration [7], and the foundation of most existing sphere decoders [6, 9] are formed by these. The F-P and S-E enumerations, and all SDs, are the QR-factorization of the channel matrix: N by $M \leq N$ matrix H with linearly independent columns factorization can be shown in factors as:

$$H = Q\begin{pmatrix} R \\ 0 \end{pmatrix} \tag{4.1}$$

Q is NxN and orthogonal, R is MxM, upper invertible and triangular, and 0 is an (N-M) xM matrix of zeros. As the objective function is invariant under orthogonal transformation, minimization problem can be written as

$$\text{argmin } s \in x^M \ |V-Hs|^2 = \text{argmin } s \in x^M \ | \left(Q^T\right) v - \begin{pmatrix} R \\ 0 \end{pmatrix} s|^2 \tag{4.2}$$

$$= \text{argmin } s \in x^M \ | \tilde{v}-Rs|^2 \tag{4.3}$$

Where $\tilde{v} = \begin{pmatrix} Q^T v \end{pmatrix}$, the lower limit 1 and the upper limit M extract the first M elements of the orthogonally transformed target.

The factored matrix of the upper triangular structure then enables the decoder to decompose the equivalent objective function (4.3) recursively as:

$$| \tilde{v}-Rs|^2 = d^2(\tilde{v}_M \ , r_{MM} s_M) + |(\tilde{v}-r_M s_M)_{\backslash M} - R_{\backslash MM} S_1^{M-1}|^2 \tag{4.4}$$

$$= d^2(\tilde{v}_M \ , r_{MM} s_M) + |\tilde{y}(s_M) - R_{\backslash MM} S_1^{M-1} \tag{4.5}$$

$$= \sum_{D=M-1}^{0} d^2(\tilde{y}(s^M_{D+1})_D, r_{DD} S_D) \tag{4.6}$$

Where the squared Euclidean distance metric is $d^2(.)$ and I have

$$\tilde{y}(s^M_{D+1}) = \begin{cases} \tilde{y}(\Phi) = \tilde{v}, & D=M \\ (\tilde{y}(s^M_{D+2}) - r_{D+1} s_{D+1})_{\backslash D+1} & D=M-1,\ldots\ldots\ldots\ldots,0 \end{cases} \tag{4.7}$$

a set of L= M-D constraint values are applied to optimization variables $ş_{D+1}\ldots\ldots\ldots\ldots\ldots,ş_M$ and parameterize the residual target. Here $\tilde{y}$ with a tilde shows that it resides in the same orthogonally transformed space as $\tilde{v}$. In this way the QR factorization provides the means of evaluating objective function efficiently. Many shared terms are contained in(4.6) summation for the decomposition. There are the values of the objective function for all B^{M-1} as in the first term of (4.5) which are involved in the search set satisfying $ş_M = s_M$. So associate the constraint $ş_M = s_M$ with this term. The (4.7) summation lends itself naturally to a weighted representation B-ary tree. It is shown in Fig.4.1 for the case where M = B = 2 and X = {-1,1}. Each of the terms in the diagram in the summations of (4.6) associated with a constraint as well as with a branch. Then each node encapsulates a set of constraints $ş_M^{D+1} = s_M^{D+1}$ and these have been applied in a way

that specified by the branches traversed along its path from the root node. A residual target can also be associated with each node by computing (4.7). I observe that the variables must be constrained in order from $ş_M$ to $ş_1$ because of the QR factorization.

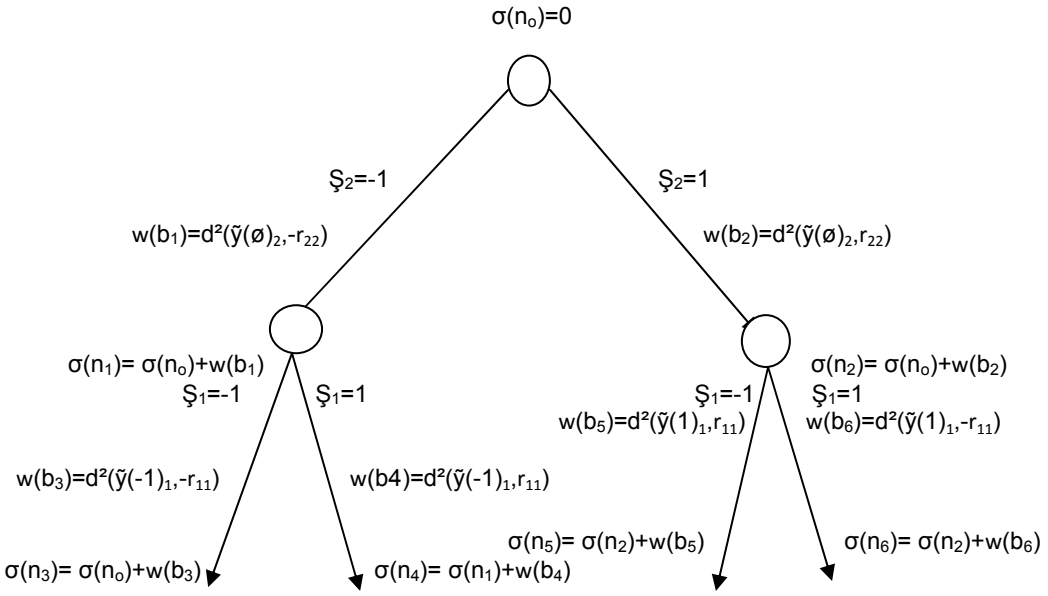

Figure 4.1: A weighted B-ary tree

with M = 2 and X = {1; 1} .

The above tree is explained by the problem parameters v, H, and X. A few properties of the tree are important to study sphere decoding algorithms.

1. Nodes are distributed over M +1 level, as the numbering from the root level node n at level 0 to the leaf nodes at M and no leaf nodes are at levels 0 through M-1.
2. Branches at levels L and L + 1 (L = 0,.....,M-1) are linked with variable $ş_D$, where I let D = M- L.
3. The B-ary, tree with each non leaf node is the parent of exactly B child. The each child branch corresponds to one of the B values in X in a way that the associated variable can take. There are B^L nodes at level L, and each is associated with a set of L constraints $ş_M^{D+1} = s_M^{D+1}$. Particularly, each leaf node is associated with a full vector of constraints $ş = s$, where $s \in X^M$ corresponds to a point in the search set.
4. This weighted tree; non-negative weights $w(b_j)$ and $б(n_k)$ are related with the branches and nodes, respectively by the proper assigning to the root node n_0 the weight 0.
5.Nodes at level L to L+1 have branches to assign weights $d^2(\tilde{y}(s^M_{D+1})_D, r_{DD}S_D)$,so that the constraints $ş_M^{D+1} = s_M^{D+1}$ are related with the parent node at level L (Property 3), and $ş_D = s_D$ is the constraint associating to the branch.
6. The summation of branch weights along the path from the root provides each node weight or as the sum of weights of its parent node and the connecting branch.
7. The node weight are not decreasing following any path from the root to a leaf node.

8. The summation (4.7) is equal to the leaf nodes weights such that these values of objective function evaluated at each of the point in the search set.

The properties 3 and 8 depict that the ML solution which is specified by the point in search set associated with the smallest leaf node weight in the tree of Fig.4.1. An exponential number of leaf nodes are considered, and in the similar way a comparable number of non-leaf nodes whose weights must all be computed in order to determine those of the leaf nodes. It is discussed in next section, how existing sphere decoders are able to reduce the number of computations from an exponential to an average case polynomial number.

4.2 The Fincke-Pohst and Schnorr-Euchner enumerations:

The smallest weight leaf node starting from the root is searched by a sphere decoder. It should start at the root and only can express itself further by computing the weights of connected branches and nodes, because of the recursive definition of the node weights. The clever pruning process of the tree, makes it able to declare an ML solution which is based on the intermediate node weights after the computation of a polynomial number of weights in the average case [70]. This is done by the property 7. Considering the geometric structure, the leaf node weight corresponds to the squared Euclidean distance from a point in the search set to the target. Points located within the sphere of radius C centred at the target can be enumerated by exploring from the root along all the branches such that node n_k is encountered as $б(nk) > C^2$. Descendents of node n_k have weights at least as б(nk) because of property 7. Therefore the point linked with the leaf nodes must lie outside of the search sphere. Then reduction of the time in computing the tree based search is done by pruning at node n_k. It means that the weights of branches and nodes which are descendants of node $n_{k,}$ need not to be computed. By traversing the tree in depth-first [75, Ch. 29] procedure, from left to right, until all nodes having weights not greater than C^2, are discovered. It returns a list of leaf nodes that relate to points located within the search sphere. This shows the behaviour of the Fincke-Pohst (F-P) enumeration with respect to the tree in Fig.4.1. The implementation can be found in works such as [76, 70]. A characteristic of the F-P strategy is that a search radius must be specified. Remember if C is too large, many node weights will have to be computed and a large number of leaf nodes may be returned. If it is too small, no leaf nodes will be found and the decoder must then be restarted with a larger search radius. These factors impact the overall computation time negatively, and so one of the main weaknesses of the F-P decoder is the sensitivity of its performance to the choice of C. Particularly the distance of the Babai point [76], is a point in the search set and it is assured to find one leaf node. Values of C and the F-P enumeration are used in the first decoder referred as the FPB. Specifically, the Schnorr-Euchner (S-E) enumeration adds a certain refinement to the F-P approach. The tree is traversed in depth first from left to right in the F-P strategy, in a way as the children of a node are considered in order of increasing $s_i \in X$, where i is the level of the parent node and recall that each of its children is linked with applying the additional constraint $ş_i = s_i$. The strategy S-E also shows that the traversing of the tree in depth- first rules instead of considering child nodes from left to right, explores in increasing order in weights according to the computation of connecting branch weights.

The S-E enumeration discovers eligible leaf nodes more quickly than that of the F-P enumeration [76]. In case if there were the only refinement, the S-E enumeration would still have to compute the same number of branch and node weights as the F-P strategy. But it is observed that as a leaf node n_l is discovered, the search radius can be adaptively reduced to $C = \sqrt{\sigma}(n_l)$. Actually after having discovered a point in the search set, I are only interested in locating those points which are even closer to the target than that point. The decoder based on the S-E enumeration has been the current state-of-the art [77-79] by adaptively adjusting the search radius.

4.3 The Schnorr-Euchner Search Order:

This search order finds quickly the estimates, ŝ, and reduces the search radius. The SE Search ordering performs a depth first search of the tree search by selecting the admissible symbol estimates, $\hat{s}_{m-k+1}$ at each level k according to an increasing distance from the unconstrained least squares estimate z_{m-k+1} given in (4.17). This was proposed in [55], [13] and rediscovered in [56]. SE search ordering represents an approach in which at each level, of the search tree first selects the symbol estimate $\hat{s}_{m-k+1}$ that minimize the metric on the left hand side of (4.14). This approach benefits as the leaf node visited by the algorithm corresponds to the ZF-DFE estimate (referred to as the Babai estimate [13]) of the transmitted message. As the ML metric in (1.4) is fairly small for the ZF-DFE estimate, the search radius will be set to a small value, limits the complexity of the search, even if the initial search radius was taken very large or even infinite. So the complexity of the algorithm when using the SE search ordering is not affected by the initial search radius (assume here that the ZF-DFE is contained within the search sphere) and the problem of selecting an appropriate search radius is eliminated. The initial search radius setting infinitely large makes it possible for the sphere decoder to obtain the ML estimate. In Paper by Fincke and Pohst [44], they considered the case of real valued vectors, matrices and integer symbols. There is a natural ordering of the elements between the lower and upper bound on the admissible symbols, $\hat{s}_{m-k+1}$ given by (4.14). The natural ordering is commonly referred to as the Pohst strategy in the communications literature [13] (investigate the branches expanding from a node in Figure4.1 from left to right). However, the adaptive radius update procedure can be applied to this case but the benefit of the radius updates is not as significant. It is recognized in the literature too that the SE ordering strategy is typically far superior to the Pohst strategy [13, 20].

4.4 An Incremental Radius:

The Pohst and SE orderings [55] is searched [20] in depth first way. It is however possible to do this in different ways, see [21] in which every conceivable search procedure is placed into a unified framework and relative benefits of various concepts are discussed. A procedure for the sphere decoder was proposed in [57], see [21] in which the equivalence between this one and stack decoder [58] is emerged where as initialization of the root node is done like other procedures. But instead of searching tree in depth first fashion, the nodes in the tree are visited in the increasing order subject to the criterion on the left hand side of (3.18).This procedure will visit the smallest set of all the search procedure to get the guaranteed one leaf node at least. The ML decision [57,

21] is obtained by the procedures of search. The set of nodes generated in this process can be easily shown that these remain the same set of nodes. These would be visited by the sphere decoder employing a certain search radius fixed. This procedure is called as the increasing radius IR which may be viewed as the sphere decoder where the radius is incremented to the tangent of the objective value of the searched node. In this case actually the sphere radius has conceptual idea rather than a pruning criteria and the sphere decoder term is not leading properly. The penalty here is that the increase in complexity is associated in finding the next node to be searched. These procedures are possibly implemented without storing the search tree. It is not possible in increasing radius IR as there is at least the part of the tree or a list of active nodes [21] must be stored in the memory. Hence IR procedure takes time complexity for the complexity of space. Future research remains to be proved as how the size of list of IR sphere decoder grows with the size of problem.

4.5 Search Algorithms:

Adopting an approach to the problem in obtaining the estimate ŝ, is the consideration of the ML detection problem. But instead of searching the entire set given by S^m only limit to some subset of S^m particularly:

$$\hat{s} = \text{argmin}_{\acute{s} \in A} ||y - H\acute{s}||^2 \tag{4.8}$$

where ($A \subset S^m$ and $|A| \ll |S^m|$).

In this case A depends on y and H. Transmitted message, s could not belong to A with non-zero probability for all $s \in S^m$ unless $A = S^m$. The value of A is explained implicitly by the algorithm that takes y and H as inputs and generates a sequence of candidates, $\hat{s}_k$ for $k = 1, \ldots, K$, as are evaluated on the basis of the ML metric. Considering from point of view, the set of possible vectors in S^m finds the detector to obtain estimate, ŝ. Clearly the error probability is limited by probability that A consists of the transmitted symbol and the complexity [51,52,53,63] is determined by the number of candidates, K, visited in the search as well as the complexity to get the next candidate in the sequence. Detector A always contains the ML estimate, $\hat{s}_{ML}$ which may be the search in as the partial search does not imply sub-optimally in terms of error of probability. In this chapter the sphere decoder is an example of the implementation. Other suggestion of detectors may be described over the possible set of the transmitted messages S^m. Examples are given by the Tabu search [39], the SAGE algorithm [40], and genetic algorithms [41]. There is another approach to perform a local search around some given, as the sub-optimal, estimate, ŝ [42].

4.6 Description of Depth-first stack-based sequential Sphere decoding algorithm:

Depth-first stack-based sequential decoding algorithm uses a decoding tree of m+1 levels where each node has 2*admissible_solution children. At each stage, the node under consideration is expanded if its weight is less than the squared distance to nearest

currently known lattice point. This distance threshold is initially set to infinity. Because it is a depth-first traversal, I expand a node by computing its first child. If it is a leaf node, clearly it cannot be further expanded. In this case, I will have found a closer lattice point than that previously known. Therefore I can adaptively reduce the distance threshold to reflect this new discovery. If the weight of the node under consideration is larger than this distance threshold, then the current search path is terminated because it cannot possibly lead to a closest lattice point. Upon path termination, the next node to be considered is the next sibling of its parent. If admissible_solution = 0, I do not apply (rectangular, or any) boundary control. In other words, optimal_det behaves as a lattice decoder. For more sophisticated operation, admissible_solution may also be a vector of length m. Then each node at the beginning of stage j in the tree, where the root node is at the beginning of stage m and the leaf nodes are found at the end of stage 1, has 2*admissible_solution(j) children. Equivalently, symbol optimal_solution(j) is drawn from {-admissible_solution(j)+1,..,-1,0,1,..,admissible_solution(j)}.If cplx = 1, I consider a tree of 2*m+1 levels with each node still having 2*admissible_solution children. In addition, either admissible_solution should be a complex-valued vector, or imag(admissible_solution) will be taken to be equal to real(admissible_solution), i.e., a square QAM constellation will be assumed by default. If either lattice reduction assistance or MMSE pre-processing are desired, these operations should also be applied in advance of calling optimal_det.

4.7 The Computational Efficiency of Sphere Decoding:

There is one of the main difficulties faced when directly comparing the computation times of different sphere decoders, for example in terms of floating-point operations, is the implementation dependent nature of this comparison. Here, I break down the operations performed by SD into three categories: expanding nodes, determining the next node to expand, and maintaining a node list. I can say that all computations involved in sphere decoding can be grouped into one of these categories. In order to provide a fair comparison, the computation time required for a single node expansion must be fixed as it should be equally optimized for all of the decoders being compared. Thus, I propose to evaluate and compare the computational performance [44,13,15,64] of the SD in a theoretical framework. I assume that this is an important characteristic for distinguishing between different decoding algorithms, and start my study of this quantity by providing a lower bound on its value.

Chapter 5 Simulation Result

5.1 System channel model:

The designed OFDM transceiver including Sphere Detection is considered operating with different QAM modulation. The full block diagram for the implemented system channel model is shown in figure 5.1. With the transceiver structure in figure 5.1 the different parts of the system are easily configurable and adaptable for parameters changes. The performance of the designed system depicted in fig 5.2 to 5.4 is evaluated by AWGN channel model for different QAM modulation including sphere detection. The Matlab simulator is constructed using a main programme holding all functions that call all parts including the transmitter and receiver models, whereas the algorithm for Sphere detection are located in a different *m* file called optimal_det.

In order to plot the BER vs. SNR for different scenarios, firstly, the bit stream is generated randomly as an input to the simulator and then it is transmitted through the implemented system. Afterwards, at the end of the simulator I compute the BER curve. This operation has been repeated several times over different values of SNR. The achieved plotted performance is compared with the theoretical performance in order to verify the correctness of the system results. Figures 5.2, 5.3, and 5.5 show the BER curves for the whole system which is depicted in fig 5.1 used for each modulation scheme i.e. QPSK, 16QAM, and 64QAM compared with the AWGN channel model. The simulations were conducted over a Additive White Gaussian Noise (AWGN), m transmit and m receive antennas. The decoders were tested by theoretical, simulated and simulated with SNR loss compensation curves for any QAM modulation technique. The experimental setup is described in more detail in fig 5.1. Among of all M-ary QAM schemes, QPSK is always has better performance in terms of Simulated curve but each symbol carries less data than that higher-order modulations does. For higher modulation schemes the SNR required for adequate operation is higher than that of QPSK. The simulated performance has more bit error rates comparing with theoretical curves even though M-QAM has higher data rates than that of QPSK. The bit error rate also increases for higher modulation with the number of bits. The intersymbol interference (ISI) and intercarrier interference (ICI) within an OFDM symbol can be avoided with a small loss of transmission energy using the concept of a cyclic prefix. The insertion of a silent guard period between successive OFDM symbols would avoid ISI in a dispersive environment but it does not avoid the loss of the subcarrier orthogonality. This problem is solved with the introduction of a cyclic prefix. This cyclic prefix both preserves the orthogonality of the subcarriers and prevents ISI between successive OFDM symbols. Therefore, equalization at the receiver is very simple. This often motivates the use of OFDM in wireless systems .First, the length of the cyclic prefix should be chosen to be a small fraction of the OFDM symbol length to minimize the loss of SNR. Because the size of the cyclic prefix is directly related to the length of the OFDM symbol or, equivalently, the number of subcarriers.The disadvantage of the cyclic prefix insertion is that there is a reduction in the Signal to Noise Ratio due to a lower efficiency by duplicating the symbol. The SNR loss is given by

$$SNR_{loss} = -10\log_{10}(S/(S + T_{cp})) \quad \ldots\ldots 5.1$$

Where S is the length of transmitted OFDM fft symbol and T_{cp} is the length of cyclic prefix. To minimize the loss of SNR, the CP should not be made longer than necessary to avoid ISI and ICI. For larger Eb/N0 values the gap between the theoretical and simulated curve increases significantly for higher modulations due to SNR loss, as the remaining equalization error becomes more significant. A loss of SNR due to the Cyclic Prefix insertion directly influence the achievable bit error rate (BER) regarding Eb/N0. However, in the BER region that is significant for most transmission systems, the system channel model performs comparable or even better than conventional transmission system, while avoiding the overhead in SNR function.

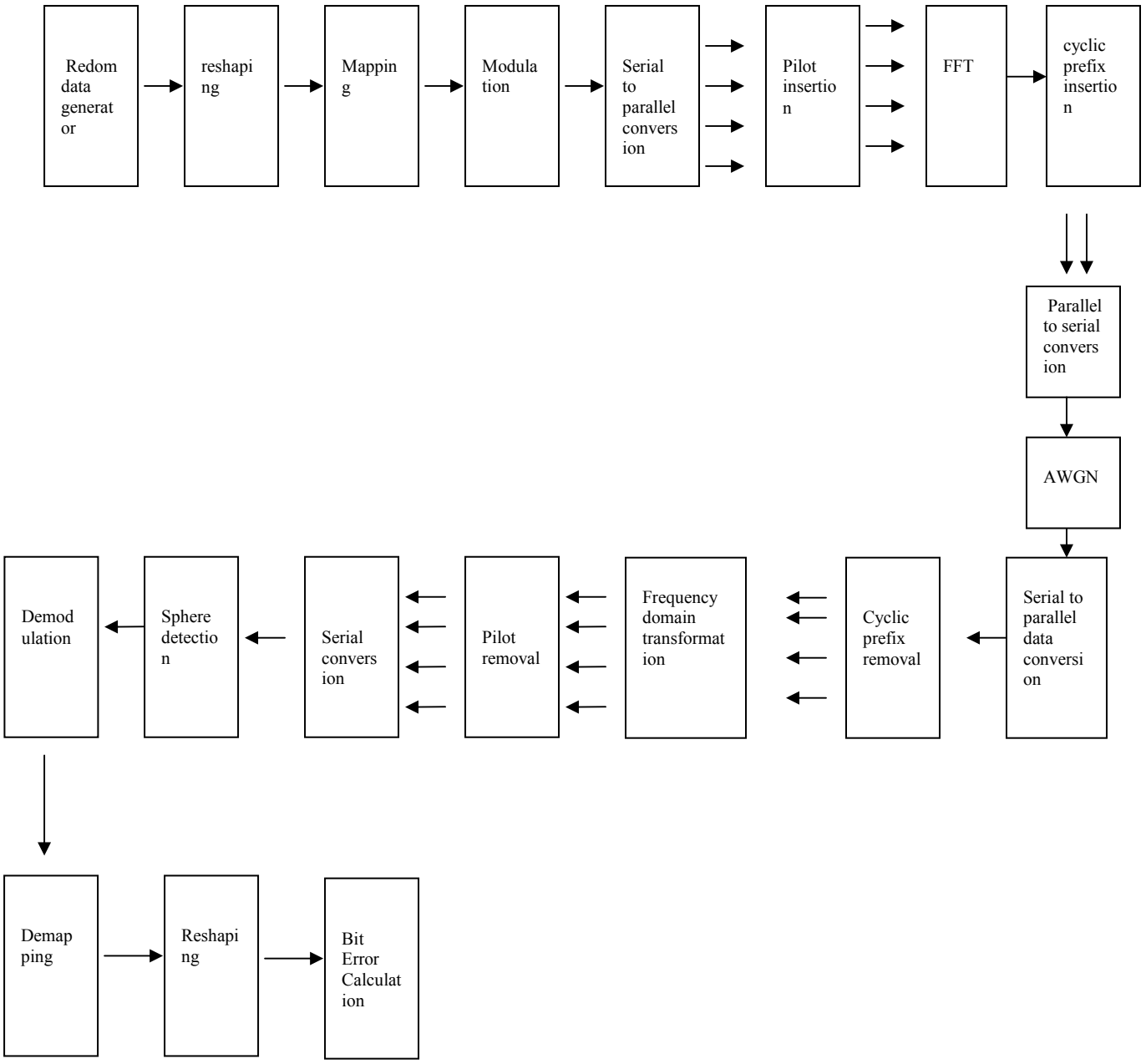

Figure 5.1: System channel model block diagram.

5.2 System parameters for performance analysis and results:

In the simulator, 20 packets of data were passed consecutively through the system channel model in which each time code word bits were passed through sphere detector. Each packet contains 5200*m bits of data where m depends on modulation scheme. To analyze the performance and the results of the designed system channel model that is depicted in figure 5.1, 20 dB of EbNo is used for theoretical , simulated and simulated with SNR loss compensation curves. The length of cyclic prefix is 16 where as the length of fft symbol is 64 having 52 subcarriers for each QAM modulation technique.

5.2.1 Performance using QPSK modulation:

Figure 5.2 respectively below shows the transceiver performance including sphere detection in terms of bit error rate (BER) after running the simulator using QPSK modulation scheme. In that output figure, both simulated and simulated with SNR loss compensation curves are plotted on the theoretical curve as the SNR and compensated SNR loss are same. The best performance is obtained comparing the result with the theoretical curve. One observable fact is that after 10 dB EbNo, the bit error rate is same for the remaining EbNo. After passing the data through the several SNR, the obtained bit error rate is within the range of .09 to .0003.

.

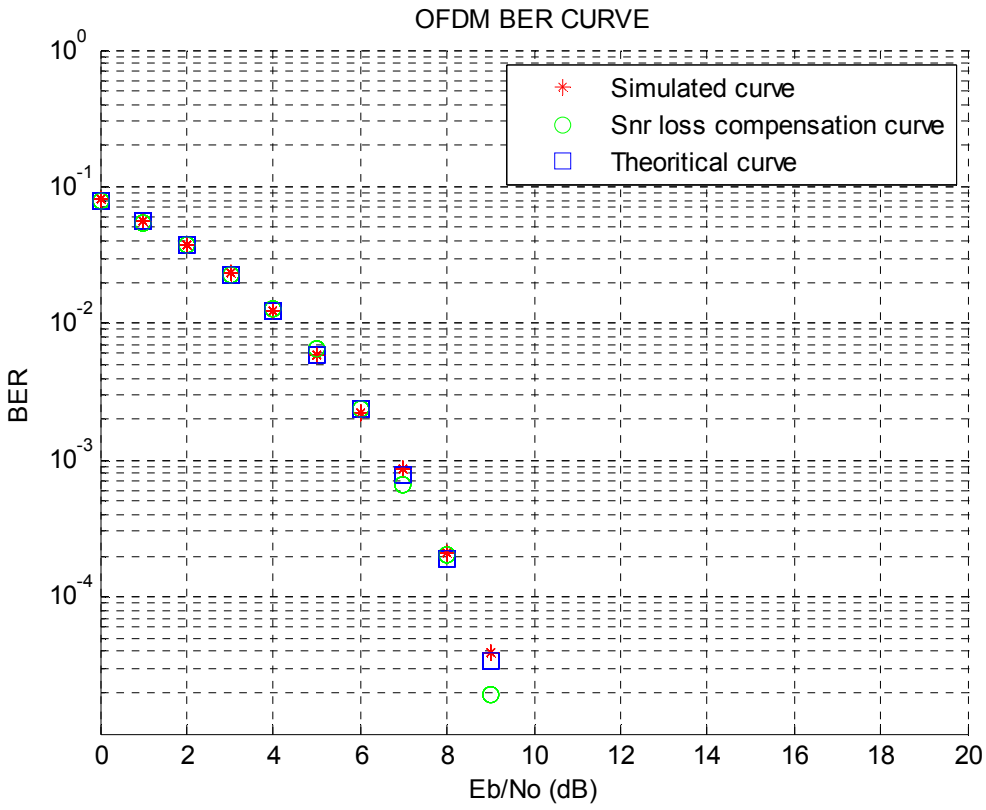

Figure 5.2: Performance analysis using QPSK modulation.

5.2.2 Using 16QAM modulation:

Figure 5.3 illustrates the performance of system in terms of theoretical, simulated and simulated with SNR loss compensation curves representing BER vs. SNR over AWGN channel model. After observation of the output figure it is clearly noticeable that the SNR loss gap between theoretical and the simulated curve increases comparatively higher than that of previous execution after 5 EbNo db due to snr loss . According to the equation 5.1, the simulated SNR loss is compensated. In the simulated with SNR loss compensated curve, a better performance is obtained than that of simulated curve. The bit error rate ranges with in .2 to .0004.

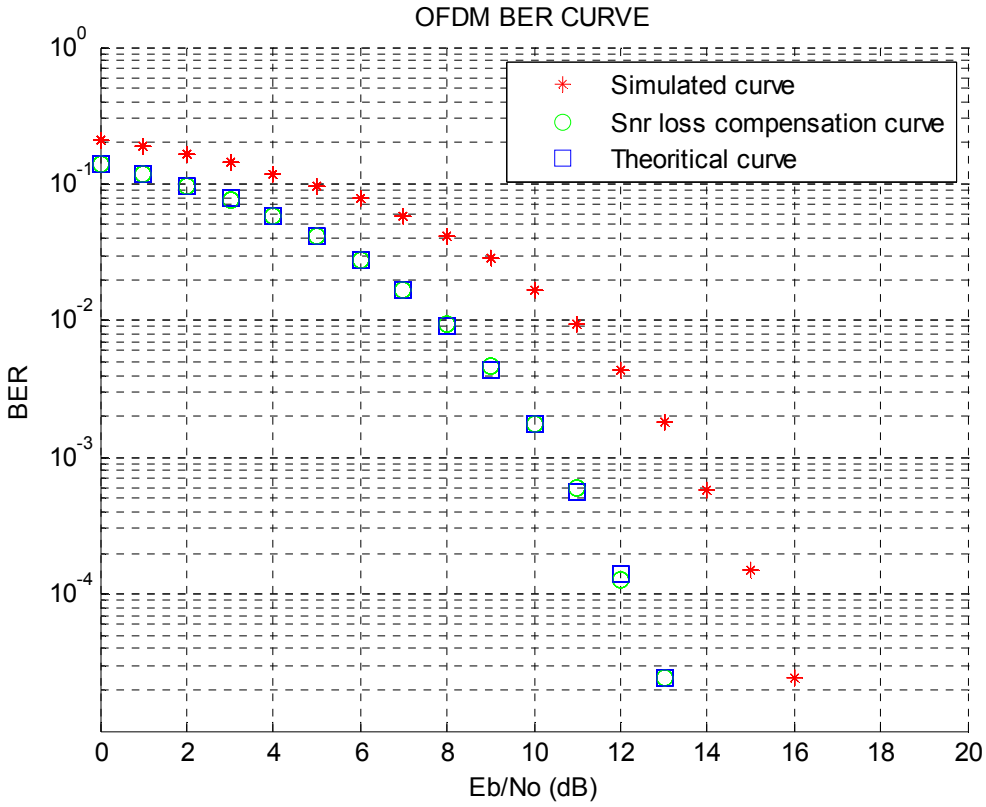

Figure 5.3: Performance analysis using 16-QAM modulation.

5.2.3 Using 64-QAM modulation:

Figures 5.4 shows the BER vs. SNR respectively, for the OFDM transceiver performance along with Sphere detection using 64QAM modulation scheme. A significant SNR loss gap is obtained for the 64-QAM modulation technique comparing with the theoretical output after 10 dB EbNo execution. The SNR loss of simulated curve is compensated according to the equation 5.1. After compensating this SNR loss, the simulated with SNR loss compensation curve is lying on the theoretical curve which

indicates the better performance comparing to simulated curve. The bit error rate of the simulated curve is with in the range of .3 to .006.

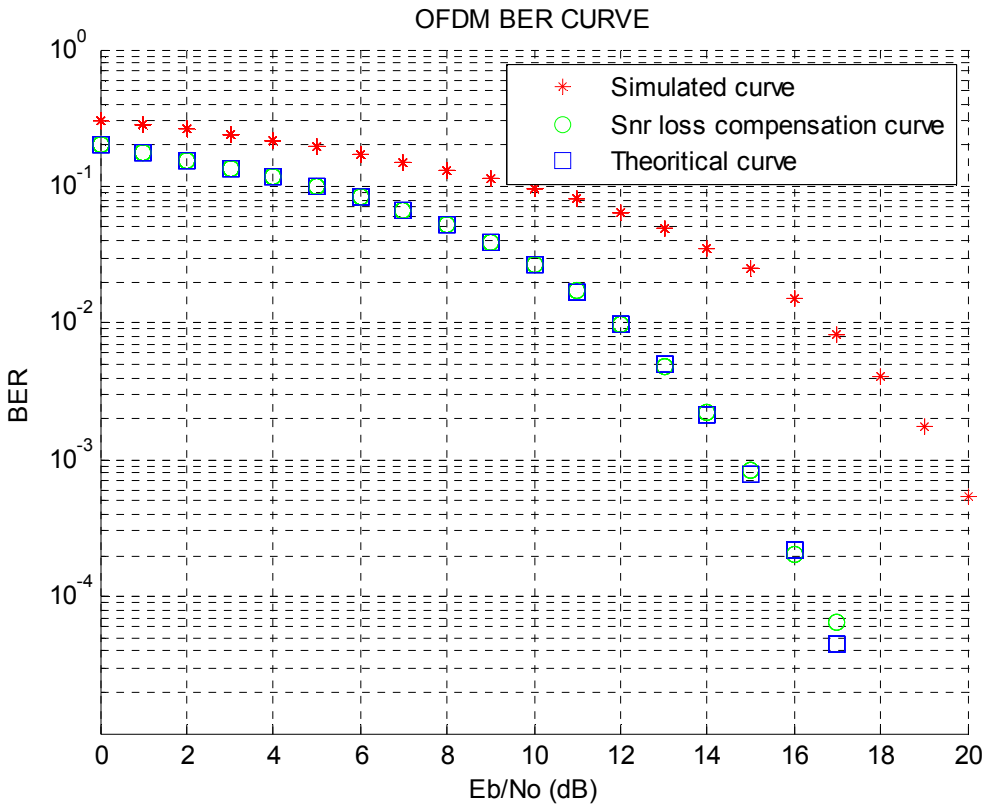

Figure 5.4: Performance analysis using 64-QAM modulation.

Chapter 6 Conclusion

OFDM is shown to be an adequate modulation technique for the future generation systems. Hence LTE that is based on OFDM, is expected to be deployed by many mobile operators in the near future. Studying the feasibility of the promising new technology OFDM by means of simulations is the main aim behind this work. It also highlights and discusses the different parts of the implemented transceiver chain. The overall performance of the implemented transceiver is given by evaluating the achieved SIMULATED BER with the theoretical one. For the future, the implemented Matlab simulator is adjustable and can be easily reconfigured for future research, for instance by considering other transmission parameters and working on other frequency spectrums. The modifications can easily take place inside the implemented simulator and to evaluate the performance of the OFDM over different spectrum allocations.

In this report I have presented a generic framework for the efficient sequential decoding algorithm .Within my framework, the problem of boundary control is handled naturally , alongside the decoding process, by means of distance threshold which is based on a closer lattice point than that previously known. Detection ordering and search radius make a statement that a large class of sphere decoder algorithms is included in that purpose. This is proven in case of detection ordering that the dependency on y in sphere decoding is a lot. Maximum eigen value of $H^{H}H$ will converge to some finite non random limit as m approaches to infinity in the case of channel matrix. Suboptimal implementation with low complexity is future research as the exponential complexity is present in the optimal sphere decoder. Sphere decoder has complexity not only in the worst case but in a probabilistic and every sense as well. This approach is given in [65, 66] as the fixed complexity sphere decoder with low error probability at high SNR and a sub exponential complexity of $O(|S|^{\sqrt{m}})$.

Appendix:

Pseudocode for the decoder:

A complete detailed pseudo code descriptions of the Sphere decoding algorithm is presented below. Assuming that the (square) upper triangular transform matrices R and P, arising from the QR factorizations of the code lattice generator G, respectively, and the border nodelist Nb are available throughout as global variables. The node data structure is defined as an 11-tuple comprising its

- weight σ in R ≥0,
- parent dimension d′ in I_n,
- parent residual target vector ỹ′ in R^{d-},
- associated vector of applied constraint values ž in $Z^{m'-d+1}$,
- position with respect to its siblings q in Z >0,
- the weight of its parent node σ′ in R ≥0
- the constraint value of its previous sibling x^- . in R ,
- parent residual translation vector ũ′ in R^{d-},
- parent residual squared radius D′ in R ≥0,
- the lower bound of its candidate range x_{min} in Z , and
- the upper bound of its candidate range x_{max} in Z .

However, instead of maintaining the nodes in a heap (or other data structure of choice), this algorithm expands these recursively. I assume that the functions are appropriately modified to return the computed child and sibling node data structures to Recursive Expand-L.

Algorithm Schnorr-Euchner Adaptive Decoder -L(v H G u D)

Input:, The channel matrix H, the target vector v the lattice generator matrix G, its translation vector u, and the squared radius D of the spherical code shaping region.

Output: The radius C of the optimal search sphere and a vector z_* .such that s.= Gz_* + u € C and $|v - Hs_*|^2 | \leq | v- Hs |^2$ and s € C , where C = (Λ(G) + u) ∩ Ś (0, D).

Pre-compute (once per LAST code):

1: $(Q_G , P) \leftarrow QR(G)$ Factor code lattice generator matrix

2: $\tilde{u} \leftarrow .Q_G^T u$ Project translation vector onto codeword space

3: $x_{min} \leftarrow \lceil (\tilde{u}_m / p_{mm}) - \sqrt{D/|p_{mm}|} \rceil$ Compute lower bound of candidate range

4: $x_{max} \leftarrow \lfloor (\tilde{u}_m / p_{mm}) + \sqrt{D/|p_{mm}|} \rfloor$ Compute upper bound of candidate range

Decode (once per received word):

5: $\tilde{v} \leftarrow Q_G^T (\tilde{u} - Ps)$ Offset and project target onto search space

6: $x_{[0]} \leftarrow v_{\_m} / r_{\_mm}$ Compute root unconstrained value
7: $x_{[1]} \leftarrow$ FirstValue-L($x_{[0]}$, x_{min} , x_{max}) Determine first candidate value
8: $\sigma \leftarrow d^2$ ($\tilde{v}_{\_m}$, $r_{\_mm}$ $x_{[1]}$) Compute weight of first child of root node
9: RecursiveExpand-L(σ , m, $\tilde{v}$, x [1] , 1, 0, x [0] , $\tilde{u}$, D, x_{min} , x_{max}) Expand first child of root
10: Return $z_* = z$ and $C := \sqrt{\ddot{y}}$

Function 2 FirstChild(σ, d′ , ỹ′, ž, ũ′, D′)

Input: The parent residual target ỹ, the weight σ , the parent dimension d′ , ′ and the constraint values ž of the node and the residual translation vector ũ′ as well as residual squared radius D′ of its parent.

Output: The border nodelist N_b (global variable).

1: d← d′-1 Determine current residual dimension
2: ũ←(ũ′ $p_{d'd'}$ - ž)\ d′ Compute current residual translation vector
3: D←D′ - d^2(ũ′$_{d'}$,$p_{d'd'}$$z_1$) Compute current residual squared radius
4: $x_{min,c} \leftarrow$ | $\tilde{u}_d$/ p_{dd} -√D/|p_{dd} | Compute lower bound of candidate range
5: $x_{max,c} \leftarrow$ | $\tilde{u}_d$/ p_{dd} +√D/|p_{dd} | Compute upper bound of candidate range
6: if $x_{max,c} \geq x_{min,c}$ then If there are any children
7: $\tilde{y} \leftarrow (\tilde{y}' - r_{-d'} \check{z}_1) \setminus d'$ Compute current residual target
8: $x_{[0]} \leftarrow \tilde{y}_d / r_{-dd}$ Compute current unconstrained value
9: x [1]←FirstValue-L(x [0] , x_{min} , x_{max}) Determine first candidate value
10: $\sigma_c \leftarrow \sigma + d^2 (\tilde{y}_{\_d}, r_{\_dd} x_{[1]})$ Compute new child node components
11: $\check{z}_c \leftarrow \left| \frac{x[1]}{z} \right|$
12: $x_c^- \leftarrow x_{[0]}$
13: Insert (σ_c , d , ỹ, $\check{z}_c$, 1, σ , x_c^- , ũ, D, $x_{min,c}$, $x_{max,c}$) into N_b Put child on border
14: end if

Function 3 FirstValue($x_{[0]}$, x_{min} , x_{max})

Input: The lower and upper bounds x_{min} and x_{max} of the candidate range of the node and the unconstrained target x [0].

Output: The constraint value x [1] of the first child node.

1: $x_{[1]} \leftarrow$ Round($x_{[0]}$) Ensure $x_{[1]} \in [x_{min} , x_{max}]$
2: if $x_{[1]} > x_{max}$ then
3: $x_{[1]} \leftarrow x_{max}$
4: else if $x_{[1]} < x_{min}$ then
5: $x_{[1]} \leftarrow x_{min}$
6: end if
7: Return $x_{[1]}$

Function 4 NextSibling(d′, ỹ′, ž ,q, σ′, x ¯ ,ũ′, D′, x_{min} , x_{max})

Input: The residual translation ũ′ and residual squared radius D′ of its parent as well as the lower and upper bounds x_{min} and x_{max} of its candidate range, the constraint values ž and the position q of the node, the weight .of its parent, the constraint value x of its previous sibling, The parent dimension d′, the parent residual target ỹ′.

Output: The border nodelist N_b (global variable).

1: if $q \leq x_{max}$-.x_{min} then If there are more siblings
2: $x_{[q]} \leftarrow \tilde{z}_1$ Get current constraint value
3: $x_{[q+1]} \leftarrow$NextValue-L(q, $x_{[q]}$, x ¯, x_{min} , x_{max}) Determine next candidate value
4: $\sigma_s \leftarrow \sigma' + d^2(\tilde{y}'_{\_d'}, r_{\_d'd'} x_{[q+1]})$ Compute new sibling node components
5: $\check{z}_s \leftarrow$ ⎪x [q+1]¡ ⎪ žl/2
6: $q_s \leftarrow q + 1$
7: $x_s \leftarrow x_{[q]}$
8: Insert (σ_s, d′ , ỹ′, $\check{z}_s$, q_s , x_s- , ũ′, D′, x_{min} , x_{max}) into N_b Put sibling on border
9: end if

Function 5 NextValue(q, x [q] , x [q -1] , x_{min} , x_{max})

Input: The lower and upper bounds x_{min} and x_{max} of its candidate range along with the position q and the constraint value $x_{[q]}$ of the node and its previous sibling x¯ .
Output: The constraint value of the next sibling node, x [q+1].

1: $x_{[q+1]} \leftarrow x_{[q]} - q$ .Sign ($x_{[q]}$ -$x_{[q-1]}$) Ensure x [q+1] € [x_{min} , x_{max}]
2: if x [q+1] > x_{max} then
3: x [q+1]←x_{max} -q
4: else if x [q+1] < x_{min} then
5: x [q+1]←x_{min} + q
6: end if
7: Return x [q+1]

Function 6 RecursiveExpand (σ, d′, ỹ′, ž, q, σ′, x ¯ , ũ′ , D′, x_{min} , x_{max})

Input: A node data structure along with the current search radius C (global variable).
Output: The current search radius C (global variable) along with the current best solution vector z (global variable).
1: if d′ > 1 then Expand node
2: $n_c \leftarrow$ FirstChild(σ, d′, ỹ′, ž, q, ũ′ , D′)
3: if σ (n_c) < C^2 then
4: RecursiveExpand(n_s)
5: end if

6: $n_s \leftarrow$NextSibling(d', $\tilde{y}'$, $\check{z}$, q, σ', $\bar{x}$, $\tilde{u}'$, D', x_{min}, x_{max})
7: if $\sigma(n_s) < C^2$ then
8: RecursiveExpand(n_s)
9: end if
10: else if $\sigma < C^2$ then Smaller weight leaf node found
11: $C \leftarrow$Sqrt(σ)
12: $z \leftarrow \check{z}$
13: end if

Bibliography

1. I.E. Telatar. Capacity of multi-antenna gaussian channels. European Transantions on Telecommunication, 10(6):585–596, December 1999.

2.G. J. Foshini and M. J. Gans.On limits of wireless communications in a fading environment when using multiple antennas. IEEE Personal Communications, 6(3):311–335, March 1998.

3. D. Tse and P. Viswanath. Fundamentals of Wireless Communication. Cambridge University Press, 2005.

4. S. N. Diggavi, N. Al-Dhahir, A. Stamoulis, and A. R. Calderbank. Great expectations: The value of spatial diversity in wireless networks. Proceedings of the IEEE, 92(2):219–270, February 2004.

5. L. Zheng and D. N. C. Tse. Diversity and multiplexing: A fundamental tradeo. in multiple-antenna channels. IEEE Transactions on Information Theory, 49(5):1073–1096, May 2003.

6. P. W. Wolniansky, G. J. Foschini, G. D. Golden, and R. A. Valen- zuela. V-BLAST: An architecture for realizing very high data rates over the rich-scattering wireless channel. In Proc. URSI International Symposium on Signals, Systems and Electronics, ISSSE, 1998.

7. A. Duel-Hallen, J. Holtzman, and Z. Zvonar. Multiuser detection for CDMA systems. IEEE Personal Communications, pages 46–58, April 1995.

8. S. Verdú. Multiuser Detection. Cambridge University Press, 1998.

9. X. Wang and H.V. Poor. Space-time multiuser detection in multipath cdma channels. IEEE Transactions on Signal Processing, 47(9):2356–2374, 1999.

10. G. Ginis and J. M. Cio.. Vectored transmission for digital subscriberline systems. IEEE Journal on Selected Areas in Communications,20(5):1085–1104, June 2002.

11. L.C. Barbosa. Maximum likelihood sequence estimators: a geometric view. IEEE Transactions on Information Theory, 35(2):419–427,March 1989.

12. T. Kailath and H. V. Poor. Detection of stochastic processes. IEEE Transactions on Information Theory, 44(6), October 1998.

13. E. Agrell, T. Eriksson, A. Vardy, and K. Zeger. Closest point search inlattices. IEEE Transactions on Information Theory, 48(8):2201–2214,August 2002.

14. H. Van Trees. Detection, Estimation, and Modulation Theory, volume 1. John Wiley and Sons, New York, 1968.

15. S. Ulukus and R. Yates. Optimum multiuser detection is tractable for synchronous cdma using m-sequences. IEEE Communications Letters,2(4):89–91, April 1998.

16. C. Sankaran and A. Ephremides. Solving a class of optimum multiuser detection problems with polynomial complexity. IEEE Transactions on InformationTheory,44(5):19581961,September 1998.

17. C. Schlegel and A. Grant. Polynomial complexity optimal detection of certain multiple-access systems. IEEE Transactions on Information Theory, 46(6):2246–2248, September 2000.

18. W.H. Mow. Maximum likelihood sequence estimation from the lattice viewpoint. IEEE Transactions on Information Theory, 40(5):1591–1600, September 1994.

19. E. Viterbo and J. Boutros. A universal lattice code decoder for fading channels. IEEE Transactions on Information Theory, 45(5):1639–1642, July 99.

20. M. O. Damen, H. El Gamal, and G. Caire. On maximum-likelihood detection and the search for the closest lattice point. IEEE Transactions on Information Theory, 49(10):2389–2401, October 2003.

21. A. D. Murugan, H. E. Gamal, M. O. Damen, and G. Caire. A unified framework for tree search decoding: rediscovering the sequential decoder. IEEE Transactions on Information Theory, 52(3):933– 953,March 2006.

22. M. Ajtai. Generating hard instances of lattice problems. In Proc. ACM symposium on Theory of computing, 1996.

23. R. Lupas and S. Verdú. Linear multiuser detectors for synchronous code-division multiple access channels. IEEE Transactions on Information Theory, 35(1):123–136, January 1989.

24. A. Kapur, C. T. Mullis, and M. K. Varanasi. On the limitation of linear MMSE detection. In Proc. IEEE International Symposium on Information Theory and its Applications, ISITA, 2004.

25. M. K. Varanasi. Decision feedback multiuser detection: a systematic approach. IEEE Transactions on Information Theory, 45(1):219–240,January 1999.

26. N. Prasad and M. K. Varanasi. Analysis of decision feedback detection for MIMO rayleigh-fading channels and the optimization of power and rate allocations. IEEE Transactions on Information Theory, 50(6):1009–1025, June 2004.

27. S. Loyka and F. Gagnon. Performance analysis of the V-BLAST algorithm: an analytical approach. IEEE Transactions on Wireless Communications, 3(4):1326– 1337, July 2004.

28. Y. Jiang, M. K. Varanasi, X. Zheng, and J. Li. Performance analysis of V-BLAST at high SNR regime. IEEE Transactions on Wireless Communications, December 2005. Sumbitted.

29. A. Yener, R. D. Yates, and S. Ulukus. Cdma multiuser detection: a nonlinear programming approach. IEEE Transactions on Communications, 50(6):1016–1024, June 2002.

30. W.-K. Ma, T. N. Davidson, K.M. Wong, Z.-Q Luo, and P.-C. Ching. Quasi-maximum-likelihood multiuser detection using semi-de.nite relaxation with application to synchronous CDMA. IEEE Transactions on Signal Processing, 50(4):912–922, April 2002.

31. S. Poljak, F. Rendl, and H. Wolkowicz. A recipe for semide.nite relaxation for (0,1)-quadratic programming. Journal of Global Optimization, 7(1):51–73, July 1995.

32. H. Wolkowicz, R. Saigal, and L. Vandenberghe, editors. Handbook of Semidefinite Programming. Kluwer Academic Publishers, 2000.

33. S. Boyd and L. Vandenberghe. Convex Optimization. Cambridge University Press, 2004.

34. H. Yao and G. W. Wornell. Lattice reduction aided detectors for MIMO communication systems. In Proc. IEEE Global Telecommunications Conference, GLOBECOM, November 2002.

35. C. Windpassinger, L. Lampe, and R. F. H. Fischer. From lattice reduction-aided detection toward maximum-likelihood detection in MIMO systems. In Proc. Wireless, Optical Communication Conference, Ban., AB, Canada, July 2003.

36. C.Windpassinger and R. F. H. Fisher. Low complexity near maximum likelihood detection and precoding for MIMO systems using lattice reduction. In Proc. IEEE Information Theory Workshop, ITW, April 2003.

37. A. K. Lenstra, H. W. Lenstra, and L. Lovasz. Factoring polynomials with rational coe.cients. Mathematische Annalen, 261:515–534, 1982.

38. M. Taherzadeh, A. Mobasher, and A. K. Khandani. LLL reduction achieves the receive diversity in MIMO decoding. IEEE Transactions on Information Theory, 2006. Submitted.

39. P. H. Tan and L. K. Rasmussen.A reactive tabu search heuristic for multiuser detection in CDMA.In Proc.IEEE International Symposium on Information Theory, ISIT, 2002.

40. L. B. Nelson and H. V. Poor. terative multiuser receivers for CDMA channels: an EM-basedapproach. IEEE Transactions on Communications, 44(12):1700–1710, December 1996.

41.C. Ergun and K. Hacioglu.Multiuser detection using a genetic algorithm in CDMA communications systems. IEEE Transactions on Communications, 48(8):1374–1383, August 2000.

42. D. J. Love, S. Hosur, A. Batra, and R. W. Heath.Chase decoding for space-time codes. In Proc. IEEE Vehicular Technology Conference,VTC, September 2004.

43. M. Pohst. On the computation of lattice vectors of minimal length,successive minima and reduced bases with applications. ACM SIGSAM Bulletin, 66:181–191, 1981.

44. U. Fincke and M. Pohst.Improved methods for calculating vectors of short length in lattice, including a complexity analysis. AMS Mathematics of Computation, 44(170):463–471, April 1985.

45. W.H. Mow.Maximum likelihood sequence estimation from the lattice viewpoint.In Proc. ICCS/ISITA,November 1992.

46. E. Viterbo and E. Biglieri.A universal lattice decoder. In Proc. 14ème Colloque GRETSI, Juan-les-Pins, France, pages 611–614, September1993.

47. O.Damen, A. Chkeif, and J.-C.Bel.ore.Lattice code decoder for space-time codes. IEEE Communications Letters, 4(5):161–163, May 2000.

48 H. Vikalo and B. Hassibi.Maximum-likelihood sequence detection of multiple antenna systems over dispersive channels via sphere decoding. EURASIP Journal on Applied Signal Processing, 2002(5):525–531,May 2002.

49.L. Brunel and J. Boutros.Lattice decoding for joint detection in direct sequence CDMA systems. IEEE Transactions on Information Theory,49(4):1030–1037, April 2003.

50.B. M. Hochwald and S. Brink. Achieving near-capacity on a multiple-antenna channels. IEEE Transactions on Communications, 51(3):389–399, March 2003.

51.B. Hassibi and H. Vikalo. On the sphere-decoding algorithm i. expected complexity. IEEE Transactions on Signal Processing,53(8):2806– 2818, August 2005.

52.B. Hassibi and H. Vikalo.On the sphere-decoding algorithm ii. generalizations, second-order statistics, and applications to communications. IEEE Transactions on Signal Processing, 53(8):2819–2834, August 2005.

53.J. Jaldén and B. Ottersten.On the complexity of sphere decoding in digital communications. IEEE Transactions on Signal Processing,53(4):1474–1484, April 2005.

54.J. Jaldén and B. Ottersten.On the limits of sphere decoding. In Proc.IEEE International Symposium on Information Theory, ISIT, pages 1691–1695, September 2005.

55.C.P. Schnorr and M. Euchnerr. Lattice basis reduction: improved practical algorithms and solving subset sum problems. Mathematical Programming, 66:181–191, 1994.

56. A. M. Chan and I. Lee. A new reduced complexity sphere decoder for multiple antenna systems. In Proc. IEEE International Conference on Communications, ICC, April 2002.

57. W. Xu, Y. Wang, Z. Zhou, and J. Wang. A computationally efficient exact ml sphere decoder. In Proc. IEEE Global Telecommunications Conference, GLOBECOM, 2004.

58. F. Jelinek. A fast sequential decoding algorithm using a stack. IBM Journal of Research and Development, 13:675–685, November 1969.

59. K. Su and I. J.Wassell. A new ordering for e.cient sphere decoding. In Proc. IEEE International Conference on Communications, ICC, May 2005.

60. A. Wiesel, X. Mestre, A. Pagés, and J. R. Fonollosa. E.cient implementation of sphere demodulation. In Proc. IEEE International Workshop on Signal Processing Advances for Wireless Communications, SPAWC, April 2003.

61. G. J. Foschini, G. D. Golden, R. A. Valenzuela, and P. W. Wolniansky. Simplified processing for high spectral efficiency wireless communication employing multi-element arrays. IEEE Journal on Selected Areas in Communications, 17(11):1841–1852, November 1999.

62. B. Hassibi.An efficient square-root algorithm for BLAST. In Proc IEEE International Conference on Acoustics, Speech, and Signal Processing, ICASSP, 2000.

63. J. A. Thomas T. M. Cover. Elements of Information Theory. Wiley,1991.

64. J. Jaldén and B. Ottersten. An exponential lower bound on the expected complexity of sphere decoding. In Proc.IEEE International Conference on Acoustics, Speech, and Signal Processing, ICASSP, May 2004.

65.L. G. Barbero and J. S. Thompson. Performance analysis of a fixed complexity sphere decoder in high-dimensional MIMO systems.In Proc. IEEE International Conference on Acoustics, Speech, and Signal Processing, ICASSP, May 2006.

66. J. Jaldén, L. G. Barbero, B. Ottersten, and J. S. Thompson. Full diversity detection in MIMO systems with a fixed complexity sphere decoder. In Proc. IEEE International Conference on Acoustics, Speech, and Signal Processing, ICASSP, 2007. Submitted.

67. 3GPP TR 25.890 V1.0.0, "High Speed Downlink Packet Access UE Radio Transmission and Reception (FDD)", (Release 5), May 2002.

68. 3GPP, “Third Generation Partnership Project (3GPP).” [Online]. Available: http://www.3gpp.org/

69.Theodore S. Rappaport, A. Annamalai, R. M. Buehrer, and William H. Tranter. Wireless communications: Past events and a future perspective. IEEE Communications Magazine, 40(5):148{161, May 2002.

70. Babak Hassibi and Haris Vikalo. On the sphere decoding algorithm: Part I, The expected complexity. To appear in IEEE Transactions on Signal Processing, 2004.

71. Emanuele Viterbo and Joseph Boutros. A universal lattice code decoder for fading channels. IEEE Transactions on Information Theory, 45(5):1639{1642, July 1999.

72. Negi, R.; and Cioffi, J.; "PILOTTONE SELECTION FOR CHANNEL ESTIMATION IN A MOBILE OFDM SYSTEM", IEEE Transactions on Consumer Electronics, Vol. 44, No. 3, AUGUST 1998

73. 3GPP TR 25.814 V7.1.0, "Physical layer aspects for evolved Universal Terrestrial Radio Access", UTRA (Release 7), 2006.

74. Jan-Jaap van de Beek, Ove Edfors, Magnus Sandell, Sarah Kate Wilson and Per Ola B.rjesson, “On Channel Estimation In OFDM Systems”, In Proceedings of Vehicular Technology Conference (VTC Ô95), vol. 2, pp. 815-819, Chicago, USA, September 1995

75. Robert Sedgewick. Algorithms. Addison-Wesley, 1988.

76. Erik Agrell, Eriksson Thomas, Alexander Vardy, and Kenneth Zeger. Closest point search in lattices. IEEE Transactions on Information Theory, 48(8):2201{2214, August 2002.

.

77. Andreas Burg, Moritz Borgmann, Claude Simon, Markus Wenk, Martin Zellweger, and Wolfgang Fichtner. Performance tradeo_s in the VLSI implementation of the sphere decoding algorithm. In IEE 3G Mobile Communication Technologies Conference, October 2004.

78.Albert M. Chan and Inkyu Lee. A new reduced-complexity sphere decoder for multiple antenna systems. In IEEE International Conference on Communications, volume 1,pages 460{464, April 2002.

79. Mohamed Oussama Damen, Hesham El Gamal, and Giuseppe Caire. On maximumlikelihood detection and the search for the closest lattice point. IEEE Transactions on Information Theory, 49(10):2389{2402, October 2003.

80. Jan-Jaap van de Beek, Ove Edfors, Magnus Sandell, Sarah Kate Wilson and Per Ola B.rjesson, “On Channel Estimation In OFDM Systems”, In Proceedings of Vehicular Technology Conference (VTC Ô95), vol. 2, pp. 815-819, Chicago, USA, September 1995

www.diva-portal.org/diva/getDocument?urn_nbn_se
http://www.essays.se/essay/b2a083f87e/
http://www.cl.cam.ac.uk/research/dtg/publications/public/ks349/Su05B

Acronyms

CDMA Code Division Multiple Access
DFE Decision Feedback
FSD Fixed Complexity Sphere Decoder
IR Increasing Radius
KKT Karush-Kuhn-Tucker (optimality conditions) [BV04]
LD-STBC Linear Dispersive Space-Time Block Code
LRA Lattice basis Reduction Aided
MIMO Multiple-Input Multiple-Output
ML Maximum Likelihood
MMSE Minimum Mean Square Error
MUD Multi-user detection
NP Nondeterministic Polynomial
PSD Positive Semi-definite
PSK Phase Shift Keying
QAM Quadrature Amplitude Modulation
SD Sphere Decoder
SDR Semi-definite relaxation
SE Schnorr - Euchner
SNR Signal to Noise Ratio
V-BLAST Vertical - Bell Labs Layered Space Time
ZF Zero-Forcing

THE END